MICROSTRUCTURAL ANALYSIS OF THE CORROSION OF Al_2O_3 AND ZrO_2 IN FRIT MELTS

A Thesis Submitted to the
Graduate School of Engineering and Sciences of
İzmir Institute of Technology
In Partial Fullfilment of the Requirements for the Degree of

MASTER OF SCIENCE

in Materials Science

By
Ceylan ŞENÖZ

July 2007
İZMİR

We approve the thesis of **Ceylan ŞENÖZ**

Date of Signature

……
Assoc. Prof. Dr. Sedat AKKURT — **20 July 2007**
Supervisor
Department of Mechanical Engineering
İzmir Institute of Technology

……
Prof. Dr. Muhsin ÇİFTÇİOĞLU — **20 July 2007**
Co-Supervisor
Head of Materials Science and Engineering Program
İzmir Institute of Technology

……
Assoc. Prof. Dr. Metin TANOĞLU — **20 July 2007**
Department of Mechanical Engineering
İzmir Institute of Technology

……
Prof. Dr. Tamerkan ÖZGEN — **20 July 2007**
Department of Chemistry
İzmir Institute of Technology

……
Assoc. Prof. Dr. Selahattin YILMAZ — **20 July 2007**
Department of Chemical Engineering
İzmir Institute of Technology

……
Prof. Dr. M. Barış ÖZERDEM
Head of the Graduate School

ACKNOWLEDGEMENT

I would like to thank the Materials Science Department at Izmir Institute of Technology for accepting me into their program and giving me the opportunity to attain an M.S degree in this field. I am greatly thankful to my advisor, Assoc. Dr. Sedat Akkurt for his patience, encouragement, and guidance during this study and my co-advisor Prof. Dr. Muhsin Çiftçioğlu for his valuable comments and suggestions.

I would like to thank to Research Assistant Mücahit Sütcü and Ceramic Laboratory Staff for their helps during my thesis study. Special thanks are to Department of Mechanical Engineering at IZTECH for providing laboratory usage and Department of Chemical Engineering, especially to Research Assistant Deniz Şimşek for conducting dilatometric measurements and Özlem Çağlar Duvarcı for the rheological studies. Also I would like to thank to Environmental Research Center (Çevre Ar-Ge) Staff, Handan Gaygısız, Esra Tuzcuoğlu, Sanem Ezgi Kınal, Filiz Kurucaovalı and Nesrin Kayırhan Gaffaroğulları, Sinan Yılmaz for their helps and patience during the ICP-AES analysis. Additional thanks are for the kind efforts and helps of İYTE Center for Materials Research Staff and to Tamsa A.Ş for providing frit samples.

Special thanks to my friends, especially to my colleagues, Elif Aras Gültürk, Suat Bahar Bozkurt, Fatma Erinç Sezgin for their friendship, help and understanding. In addition, special thanks to Dr. Bora Derin for providing some of the phase diagrams in FactSage programme at İstanbul Technical University.

I would like to thank especially to my family for their support and understanding.

ABSTRACT

MICROSTRUCTURAL ANALYSIS OF THE CORROSION OF Al_2O_3 AND ZrO_2 IN FRIT MELTS

Dense alumina and zirconia crucibles manufactured in the laboratory by slip casting were tested for their resistance to corrosive attack by opaque and transparent frits between 1400-1500^{o}C. Interface between the crucible and the frit was investigated by Scanning Electron Microscopy (SEM, Philips XL-30S FEG) equipped with EDS (Energy Dispersive Spectroscopy) unit, X-ray diffraction (XRD, Philips X'Pert Pro), and Optical Microscope (OM, Nikon Eclipse L150). Formation of a continuous band of zinc aluminate (gahnite) crystals was observed at the interface between the alumina crucible wall and the contained opaque and/or transparent frit melt. When opaque frit was used, isolated pockets of zirconia were present adjacent to the zinc aluminate band inside the frit. Deeper inside the frit incompletely dissolved zircon were observed. On the other hand zirconia crucible failed against both of the corrosive frits, resulting in complete penetration of frit species into zirconia crucible wall. Thermodynamic predictions based on the use of phase diagrams also produced similar conclusions with the practically observed results. Crucibles with 50 wt% zirconia and 50 wt% alumina were also manufactured and tested for their corrosion resistance against the frit. It was found that the alumina crucibles could be safely used for corrosion testing with minimal aluminum contribution to the frit melt.

ÖZET

Al_2O_3 VE ZrO_2'NIN FRİT ERİYİĞİ İÇERİSİNDEKİ KOROZYONUNUN MİKROYAPISAL ANALİZİ

Laboratuvarda slip-döküm yöntemiyle üretilmiş olan yoğun alumina ve zirkonya krozelerin 1400–1500 ^oC aralığında opak ve saydam frit korozyonuna dayanımı test edilmiştir. Kroze ve frit arasındaki arayüzey SEM-EDS, XRD ve OM yöntemleri kullanarak incelenmiştir. Devamlı bir bant şeklinde $ZnAl_2O_4$ kristallerinin oluşumu Al_2O_3 kroze duvarı ve içeriğindeki opak ve/veya saydam frit eriyiği arasındaki arayüzeyde gözlemlenmiştir. Opak frit kullanıldığı zaman izole olmuş ZrO_2 kümeleri $ZnAl_2O_4$ bantına komşu bir şekilde frit içerisinde oluşmuştur. Frit yüzeyinde daha içerilere girildiğinde ise çözünümünü tamamlamamış $ZrSiO_4$ gözlemlenmiştir. Öte yandan ZrO_2 kroze her iki aşındırıcı frite karşı, fritin ZrO_2 kroze duvarına tamamen nufuz etmesi nedeniyle başarısız olmuştur. Faz diyagramlarının kullanımı üzerine olan termodinamik tahminler de pratikte saptanan sonuçlar ile benzerlik göstermiştir. Ayrıca, kütlece 50% zirkonya ve 50% alüminadan oluşan krozeler de üretilmiş ve frite karşı korozyon dayanımları test edilmiştir. Alümina krozelerin, frit eriyiğine minimum alüminyum katkısı ile korozyon testi için güvenle kullanılabileceği sonucuna varılmıştır.

TABLE OF CONTENTS

LIST OF FIGURES

Table **Page**

LIST OF TABLES

Table **Page**

CHAPTER 1

INTRODUCTION

Ceramic products are made from natural or synthetic raw materials and are generally characterized by their high hardness and melting point combined with low toughness and resistance to fracture. They are the combination of complex oxides and silicates, also useful carbide, nitride, and boride ceramics are produced. Their stable properties depend on their structurally strong bonding. This stability protect materials from the attack of strong acid and high temperature corrosive gases and liquid metals. In addition, great hardness and high melting temperatures are led by this strong bonding.

Refractories are ceramic products that can withstand high-temperature corrosive conditions encountered in industrial furnaces and process vessels. Furnace linings, crucibles, molten metal ladles, and other special high temperature products are manufactured from refractory materials. So, refractories must have good hot strength, high melting temperatures, chemical attack resistivity and resistance to abrasion. A flow sheet for manufacturing refractories is shown in Figure 1. (Jones et al. 1993).

Some of the refractories that are used in frit kilns are suffering from excessive corrosion. Improper choice of refractories results in production losses and sometimes even catastrophic shut-downs (McCauley 1996). A corrosion testing protocol is therefore necessary to help ceramics manufacturers to identify the correct type of refractories for their furnaces.

Crucibles are popular materials used in the laboratory for melting different types of solid samples at varying high temperatures. Their use cannot be avoided. Oxides are ideal materials for such applications because of their inherent thermal and chemical stability. In a separate project that was recently started a large number of laboratory crucibles were needed. Potential crucible materials that could be produced in-house were investigated for their thermodynamic compatibility and speed of manufacture. However, choice of the crucible material largely depends on the chemical environment and the processing temperature. The high melting points and resistance to chemical attack of several pure oxides make them useful as crucible materials. Platinum crucibles are generally used for melting soda-lime-silicate glasses (Mazer et al. 1991). They are, however, costly and difficult to clean. Leigh et al. state that ceramic crucibles can

conveniently be used as a consumable to be replaced after each run (Leigh et al. 1987). On the other hand, there is a tendency of ceramic crucible materials to dissolve into the processing liquid which is in this study a molten frit bath. This type of dissolution can perhaps jeopardize the accuracy of the corrosion test which relies on the chemical stability of the frit melt (Dunkl et al. 2003). It is therefore important to use ceramic crucibles which will show the least amount of dissolution and chemical interaction with the frit melt.

The goal of this study is to develop laboratory crucibles from different ceramics for use in corrosion testing of frit furnace refractories and to investigate interactions between frit melt and crucible. So, two types of frits were the melts that were aimed for containment. Initially, phase diagram study was performed to name the potential crucible materials to resist against these melts and to predict the degree of corrosive attack. In addition to the chemical resistance, crucible materials must be free from phase transitions that may lead to undesired volume expansions/contractions or perhaps even cracking during the heating and cooling cycle of the corrosion test. Obviously the crucibles must be completely dense to avoid liquid penetration and to minimize the surface area offered for corrosive reactions. Dense ceramics can be produced via isostatic pressing, plastic forming, ram pressing or slip casting. Hence, not only the above chemical criteria must be met for proper crucible material selection, but also the processing technique must be carefully evaluated. In order to achieve full density of the crucible, a fine particle size of the starting powder is necessary to produce the desired driving force for sintering at practically low temperatures which were in this study around 1550^{o}C.

This thesis includes the following subjects: materials used in the production of laboratory crucibles, processing techniques for ceramics, forming rheologically stable suspensions and characteristics of frit species are mentioned in Chapter 2. In Chapter 3, corrosion phenomena and phase diagrams used in this study are discussed. The experimental procedure and the results of this study are given and discussed in Chapters 4 and 5 whereas the conclusions related to the recent study and the future work recommendations are stated in the last chapter.

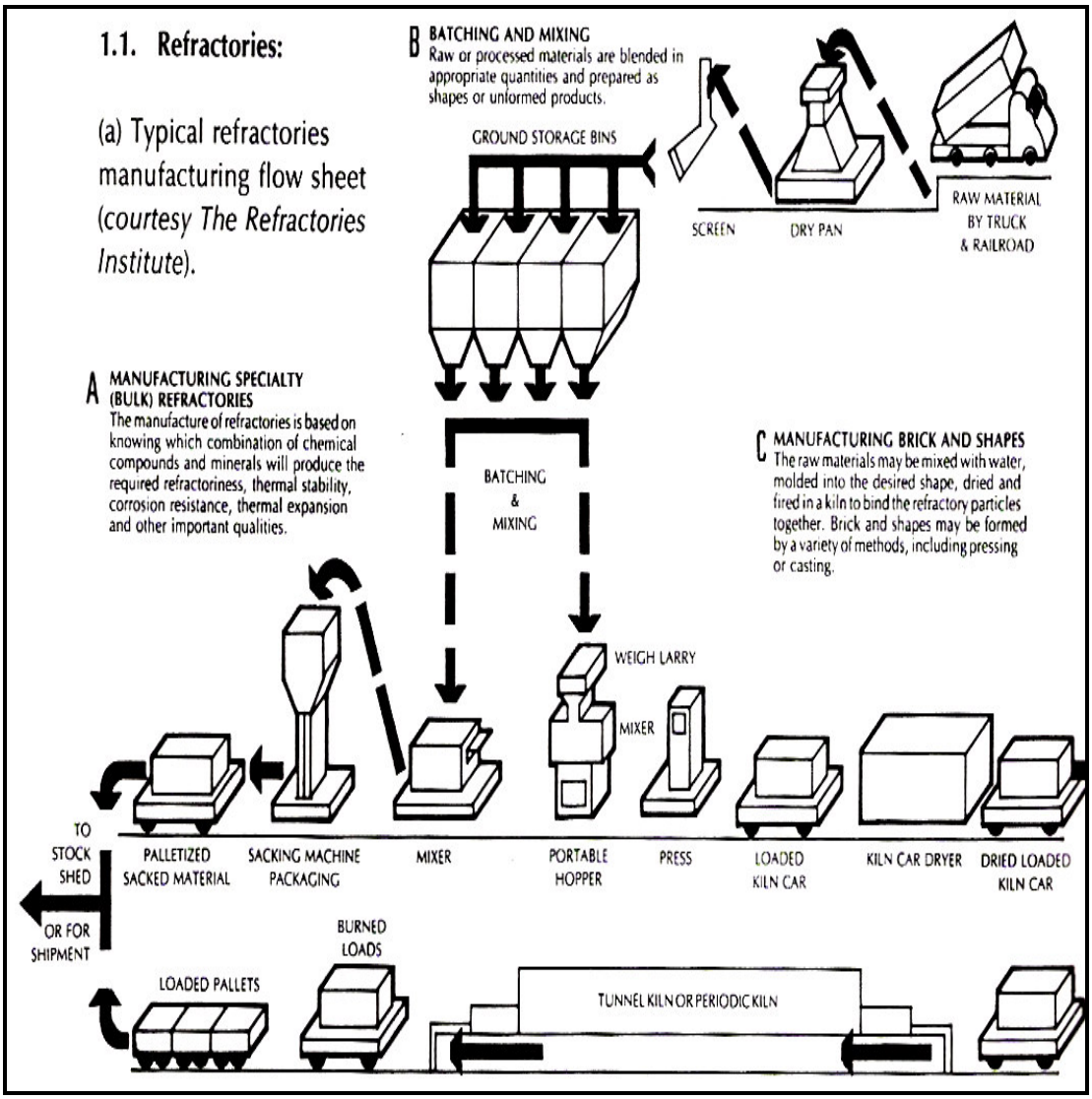

Figure 1. Typical refractories manufacturing flow sheet.

(Source: Refractories Institute 1993)

CHAPTER 2

CRUCIBLES AND FRIT

In this chapter, materials used in the production of laboratory crucibles, forming rheologically stable suspensions and processing techniques for ceramics will be briefly explained.

2.1. A General Look at the Materials Used in the Production of Crucibles

Crucibles, one of the most useful laboratory equipments for high temperature applications, can be either metallic/alloy or ceramic. The choice of the appropriate material mostly dependent on the chemical interaction between the processing liquid and the crucible material, meaning that there must be a tolerant dissolution between both species. Also the reaction temperature plays an important role in the selection of the proper crucible, as the material is expected to withstand to that temperature without undergoing phase changes. Table 2.1.1. displays the usual crucible materials and their properties.

Table 2.1.1. Usual crucible materials and their properties.
(Source: R.F. Bunshah 1968)

Material	**Melting or softening temperature (°C)**	**Typical charge**	**Atmosphere**
Quartz	1600	Ge, Si	inert, oxidising, reducing
Alumina	2050	Al, Fe, Ni, Co, Pd, Pt Ag,	inert, oxidising, reducing
Magnesia	2800	as in alumina, plus Mn	inert, oxidising, reducing
Stab. zirconia	2200		inert, oxidising, reducing
Graphite	>3000	Al, Bi, Cd, Au, Ag	inert
Boron nitride	2100	Zr, Hf	inert, oxidising,reducing
Platinum	1650	oxides, glasses	inert, oxidising
Iridium	2410	oxides	inert, oxidising, reducing

In the manufacture of technical ceramics, such as in manufacturing crucibles, alumina (Al_2O_3) is used extensively. It is an excellent electrical insulator and abrasive, in essentially pure form. And its high melting point (2050 ^oC, 3722 ^oF) makes it a popular refractory. Graphite is one of the useful material to be used in manufacturing crucibles due to its superrefractory properties. It can be used in processes held at the highest industrial temperature and generally not wetted by melts and slags, meaning that excellent resistance against chemical attack. Zirconia (ZrO_2) and zircon ($ZrSiO_4$) are important refractory materials acting as excellent thermal insulators. On the other hand, possible phase changes through reaction temperature are an issue. For example ZrO_2 change from monoclinic to a tetragonal phase at 950 ^oC. This phase transition of ZrO_2 results in a 3–5 % change in volume, which causes cracking of the ceramic crucible when the temperature of the furnace is kept constant in that temperature region (Pretorius 1995).

Metal crucible use in fast firing applications is frequent depending on the low specific heat capacity and high thermal conductivity values. Having high melting points above the process temperature is also an advantage whereas the possibility of reacting with oxygen or any other medium gases in the furnace is a drawback.

The processing liquid under study may be a molten metal as well as a molten glass. Poirier et al. studied the corrosion of andalusite-based refractories by corrosive steel making slags in high-alumina crucibles (Poirier et al. 2004). On the other hand, Akamatsu, used a quartz double crucible in the fabrication of a phosphate glass fiber (Akamatsu 1983). Where as alumina, tin oxide and zirconia crucibles were tested for one of the heavy metal oxide glasses, $PbO\text{-}Bi_2O_3\text{-}Ga_2O_3$ glasses (Santos et al. 2002) .

Phase diagrams are of technical significance for sintered ceramic materials, traditional porcelains and also for glass ceramics. In this study the selection of the crucible material was based on the use of three component phase diagrams that most closely covered the composition of the processing liquids and the crucible. Through the phase systems in consideration, any presence of liquid phase in the contact area of the species was not observed, as this gives noteworthy idea on whether penetration is allowed through the grains or not. To sum up, the produced crucible must be: resistant to high temperatures, impervious, chemically as inert as possible, mechanically strong enough and have large grain size.

When the composition of the processing liquid and the reaction temperature are considered, the best materials to be used to produce crucibles in this study are identified

as alumina, zirconia and alumina-zirconia mix material. The next part includes the possible processing methods for ceramics.

2.2. Processing Methods for Ceramics

In a particular application**,** depending on the requirement of the component, fabrication methods may vary. The cost of fabrication strongly affects the choice of a particular fabrication method. In addition, the forming procedures for advanced applications of ceramics require special care in order to ensure minimum defect levels (especially microcracks, voids and surface pits). When formation of ceramic parts and metal parts are compared, it is obvious that to form ceramics is more diffucult than to form metal parts as ceramics have characteristics such as inherent brittleness, hardness, and high melting temperatures in general.

On the other hand, especially in the production of ceramic crucibles, homogeneous distribution of the particles is required in order to obtain a high-density impervious product. So, this must be the criterion of top priority in the choice of processing method to be used in the production of crucibles. The expanded list of processing methods used in technical ceramic manufacturing is given below:

2.2.1. Isostatic Pressing

Pressing can be classified depending on the direction of pressure application, that is uniaxial or isostatic. One of the ideal dry forming method in which pressure exerted uniformly on all surfaces of the powder mass and throuhgout the formed part is isostatic pressing. A dry or semidry granulated ceramic mix is placed in a pliable rubber or polymer mold, which is sealed, evacuated, and then sequeezed uniformly by immersion in a high pressure oil or water cylinder. Typical pressures are 280MPa. (Ceramics Industrial Processing and Testing, Second Edition 1993).

2.2.2. Slip Casting

The success of slip casting process depends on two main factors: slip and the mold. A slip is slurry of very fine ceramic materials suspended in water (or occasionally another liquid) and generally having the consistency of thick cream. Starting with the treatment of slip and/or slurry, it can be concluded that the casting behaviour of it, depends strongly on gelling behaviour (change of viscosity with time). In order to control the flow properties of slips, additives are used for the dispersion of agglomerates, in other words, flocs. So, these additives are also named as deflocculants as they break up the agglomerates. Sodium silicate, sodium carbonate, sodium phosphate, and a number of organic substances such as the polyacrylates are common deflocculants used with slips.

As mentioned above, the preparation and care of plaster molds is another factor effective on the success of a slip casting operation. The strenght and porosity of the resulting molds are determined with the amount of setting water used in mixing the plaster. In slip casting, water is removed from the powder suspension by the water suction of the plaster mould and a consolidated layer consisting of packed particles builds up. When a desirable thickness has been reached the excess slip is removed (drain casting) , or the casting proceeds until the casting fronts approach each other and a solid body has been obtained (solid casting), (Figure 2.2.). In this manner a ceramic article (cast) can be formed having outer configuration that reproduces the inner configuration of the plaster mould (Ceramics Industrial Processing and Testing, Second Edition 1993).

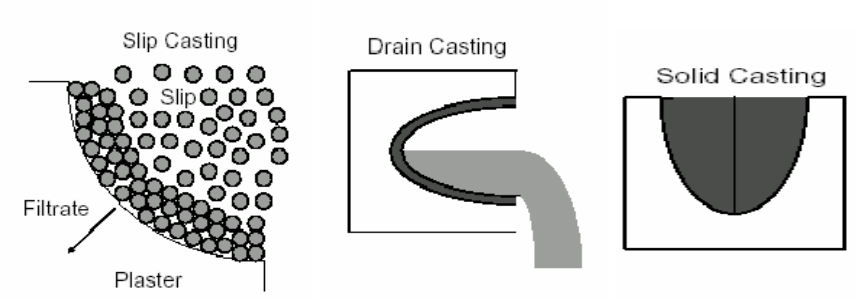

Figure 2.2. Slip casting schematically.
(Source: WEB_1, 1997)

Slip-cast products are less porous than those shaped by plastic processes, but their dimensional uniformity is only average.

2.2.3. Ram Pressing

Another plastic forming technique is RAM pressing. It is typically used to form large platters such as large floor tile. Modern RAM pressing uses a hydraulic press with two porous or permeable dies to form the finished shape. These have typically been made of gypsum cement (plaster), sometimes reinforced by metals. A bat of plastic material is placed on the lower mold and pressed to shape by the upper mold during RAM pressing. In order to remove the part, air is applied behind the lower mold. The air passes through the mold material and gently blows the part free. The part stays with the upper mold and then, when the upper mold is at its raised position, is released onto a tray or holder by application of air pressure behind and through the upper mold (Dry Pressing Technical Ceramics, The American Ceramic Society Bulletin 1996).

2.2.4. Pressure Casting

Pressure casting is a generic term to specify a fabrication technique where solidification is promoted under high pressure within a re-usable die. This process is similar to injection molding, a variant of porous mold casting. The ceramic suspension is injected into the mold under high pressure (Ceramics Industrial Processing and Testing, Second Edition 1993).

2.2.5. Dry Pressing

This method is particularly well-suited for the rapid production of various ceramic parts in which the granulated powder is placed in a steel die under very high pressures. The process is sometimes referred as dust-pressing, die-pressing, or uniaxial-compaction. This is a cheap process used for the production of porcelain tile, cutting tools, grinding wheels, chip carriers, refractories, insulators, seal rings and nozzles. (Ceramic Microstructures 1994).

2.2.6. Gel Casting

One of the useful ways of forming ceramic materials is gelcasting. It is a method in which ceramic powders are molded into green products with the presence of a monomer solution that is used as a binder vehicle and the controlled polymerization of the monomer in solution serves as a setting mechanism. The resulting green product is of exceptionally high strength and may be dried to remove water. After drying, the product may be further heated to remove the polymer and may also subsequently be fired to sinter the product to a high density (Janney et al. 1992).

2.2.7. Tape Casting or Doctor Blade forming

This process utilizes a suspension of ceramic particles in a liquid. The flow ability of the suspension is similar to a slip casting suspension, but the slip used in tape casting contains a higher content of an organic binder. A smooth, flat surface is required for pouring or spreading the slip in order to form a thin film typically under 2 mm thickness. The fluid is removed by heat or flowing air in order to leave a thin tape consisting of moderately close-packed ceramic particles bonded together by the organic binder. As the tape is flexible, it can be cut, punched, metallized. Machines used in tape casting process are called “doctor blades” , those are whether stationary blade/moving carrier machines or moving blade/stationary carrier machines (Richerson et al. 1989).

2.2.8. Injection Molding

In this cyclic process known as injection molding, granular ceramic powders are first mixed with resin binders and special plasticizers. Then this mix is heated until softened and forced into a mold cavity where it cools and resolidifies to produce a part of the desired shape. Chemical manufacturers formulate special resins in order to optimize the process. Spark plugs, ceramic cores, thread guides, electronic parts, welding nozzles, and dental braces are succesfully produced by injection molding (Mutsuddy et al. 2000).

2.2.9. Extrusion

Materials those having an axis normal to a fixed cross section, such as bricks, sewer pipes, hollow tiles, technical ceramics and electrical insulators are produced by this method. A stiff plastic mix through a die orifice is extruded. In order to eliminate air bubbles, the most widely practiced method is to use a vacuum auger, throughly mix the body with 12 to 20 % water and force it through a hardened steel or carbide die. The net shape and continous forming competences of the extrusion process are very attractive (Kingery 1976).

2.3. Preparation of Stable Ceramic Suspensions

In this study slip-casting method was decided to be used to form one of the most widely used technical ceramic type, crucibles, in laboratory conditions after evaluating the cost and the convenience through the given methods.

As mentioned earlier, the slip-casting method has two requirements, first is the preparation of a proper plaster mold, second a stable slip as the most undesired situation in slips is the thixotrophic behaviour of the system. The best materials to be used to produce crucibles were identified as alumina, zirconia and alumina-zirconia mix. So, through literature research, priority was given to techniques used in the preparation of alumina, zirconia and alumina-zirconia slurry and/or slip. In order to have optimum slip compositions, several trial slurries and/or slips of each material (alumina and/or zirconia) were prepared to evaluate between the best suspension.

2.3.1. Alumina Suspension Preparation

Most of the literature studies point out the use of Darvan-C as a deflocculant in the preparation of alumina suspensions. Singh et al. have investigated the electrokinetic and adsorption characteristics of alumina suspensions in the presence of Darvan-C as dispersant and as a result of electrokinetic studies they concluded that alumina particles are positively charged (Singh et al. 2004). By the adsorption of polyelectrolyte, the charge on the particles becomes more negative. On the other hand, Popa et al., claim that without base addition, Darvan-C is not completely dissociated (Popa et al. 2006).

As ethanol is a slightly acidic solvent, the Al_2O_3 particles in ethanol are slightly positively charged. The adsorption mechanism is developed by electrostatic attraction between the $–COO^-$ groups and the positively charged surface hydroxyl sites of alumina. In this case, according to Tang et al., the adsorption is of the high affinity type and the polyelectrolyte will be adsorbed on the surface until saturation (Tang et al. 1998). All of the mentioned studies show that Darvan-C is a compatible deflocculant in the dispersion and stabilization of alumina particles. Whereas, Pradhan suggests that the addition of sucrose has an influence on the decrease in the many rheological properties of the 35 and 45 vol.% alumina slurries, such as in apparent yield stress, viscosity, thixotrophy, and increase in non-Newtonian index as compared with the slurries prepared just using the polyacrylate, also creates a weakening in the inter-particle network (Pradhan 2005). Zhang's work, suggests that although polyacrylic acid (PAA) is known to be an effective dispersant for Al_2O_3 powder in aqueous media, its influence is insuffient at high solids loading (> 55 vol.%). As the dispersion of the Al_2O_3 suspensions becomes difficult when only PAA is used as a dispersant, ethylenediamminetetraacetic acid, tetrasodium salt, dihydrate (EDTA-4Na) was introduced to improve the dispersion of the Al_2O_3 suspensions (Zhang et al. 2006). Briscoe et al., state that in both rheological and sedimentation studies, the three commercial dispersants "Darvan C", "Aluminon" and "Tiron", which have been investigated with respect to their effect on the stabilization of the alumina AES-11 suspension were found to be capable (Briscoe et al. 1998). Also, some viscosity measurements were conducted by Haake Mars Modular Advanced Rheometer, Germany in plate and plate mode in order to see the effect of solids loading.

2.3.2. Zirconia Suspension Preparation

In the case of the preparation of the zirconia slips, according to Zhang et al., the slurry stability is achieved by the use of a commercially available dispersant, Triton X-114 and the results showed that it is an effective dispersant in preparing stable zirconia suspensions (Zhang et al. 2006). Leong et al., claim that the rheological properties of concentrated ZrO_2 suspensions have been shown to be strongly affected by pH and anion type. At high pH, the ZrO_2 suspensions were dispersed by KOH, while hydrochloric or nitric acid can be used for dispersion at low pH (Leong et al. 1990). The

study shows that in order to prepare stable zirconia suspensions of the desirable rheological properties, a good understanding of surface chemistry is required. Havrda et al., state as good dispersion at high solids loading is not only necessary but a pre-requisite for all slurry based forming techniques, it is critical to be able to increase the solids loading in the slurry to as high a level as possible (Havrda et al. 2004). In that study for the optimization of rheological properties of a TZ-3Y (by TOSOH Corp. Japan) zirconia suspension, 77 wt.% solids loading and different amounts of commercial dispersant, Dolapix CE-64, alkali free, carboxylic acid (Zschimmer & Schwartz, Germany) were used with the controlled viscosity measurements. Also, in order to select the best deflocculant to prepare a stable ZrO_2 suspension, an experimental design, twelve-run Plackett-Burmann screening design was applied. Plackett-Burman designs are a class of screening, two-level fractional factorial designs that are often used to study main effects. The advantage of screening designs is that, the important factors, main effects, considered are screened out among the other factors and the number of experiments made is at minimum. There is obviously tremendous reduction in experiments by using a Plackett-Burmann design. In this study, depending on the number of factors (deflocculant types), twelve suspensions were prepared. Low viscosity and high constant ZrO_2 powder use in each suspension with different deflocculant volume were the selection criteria. However, Sarraf states that the bulk density of high solid content of zirconia slips (77 wt. %) with the addition of 1.4 wt. % Dolapix CE-64 is observed to be stable (Sarraf 2004). He also observed lower apparent porosity,open porosity and water absorbtion in green state.

2.3.3. Alumina-Zirconia Suspension Preparation

Alumina toughened zirconia ceramics with e.g. 20 wt.% Al_2O_3 (ATZ) appear to be perspective competitors in ceramic industry. High values of mechanical strenght and fracture toughness are among the main advantages of these ceramic materials. Kunes et al., state that in the case of producing a bioceramic material by slip casting, a stable, agglomerate-free suspension with almost newtonian flow behavior is one of the basic requirements (Kunes et al. 1999). In this work suspensions of three commercial zirconia powders with different alumina admixtures (Tosoh TZ-3Y, TZ-3YE, TZ-3Y20A) were investigated.

Rotational viscometry was used in order to determine the rheological behavior. For the stabilization of the aqueous suspensions: Dolapix CE64 and Dolapix ET85 (Zschimmer & Schwarz, Lahnstein / Germany) and Sokrat 32A (Chemické závody Sokolov / Czech Republic) were the three frequently recommended deflocculants. For all the three powder types, alkali-free polyelectrolyte Dolapix CE–64 turned out to be the most effective deflocculant with an optimum concentration of 0.6 wt.% in all cases.

Garrido et al., studied powder compositions with different alumina/zircon (wt.%) ratios in the mixtures and effect of chemical composition with the addition of polyacrylate. Simultaneous dispersion of the powders at pH 9.1–9.2 by addition of 0.2–0.24 wt.% polyacrylate resulted in a well-dispersed suspension showing a minimum in viscosity (Garrido et al. 2001).

On the other hand for the production of AZ crucibles, Frederici et al., prepared aqueous slips which were slip-cast by direct ball milling of a mixture of the oxides Al_2O_3/ZrO_2 for 12h in alumina jars with alumina balls and water and ammonium polyacrylate was used as deflocculant in the preparation of slips (Frederici et al. 2000).

2.4. Frit

Frit, solid granules (Figure 2.4.1a-b.) simply termed glass, is obtained by mixing two or more raw materials fused together and cooled rapidly in order to be used in the preparation of glaze. Frit species are used in glazing porcelain and pottery also in enameling iron and steel. Enamels used in porcelain industry are glassy coatings fused onto metals in order to avoid corrosion and provide decoration. The other industrial applications of frit can be summarized as follows: to lower vitrification temperatures, in bonding grinding wheels and as lubricant in steel casting and metal extrusion. (Berard et al. 1993).

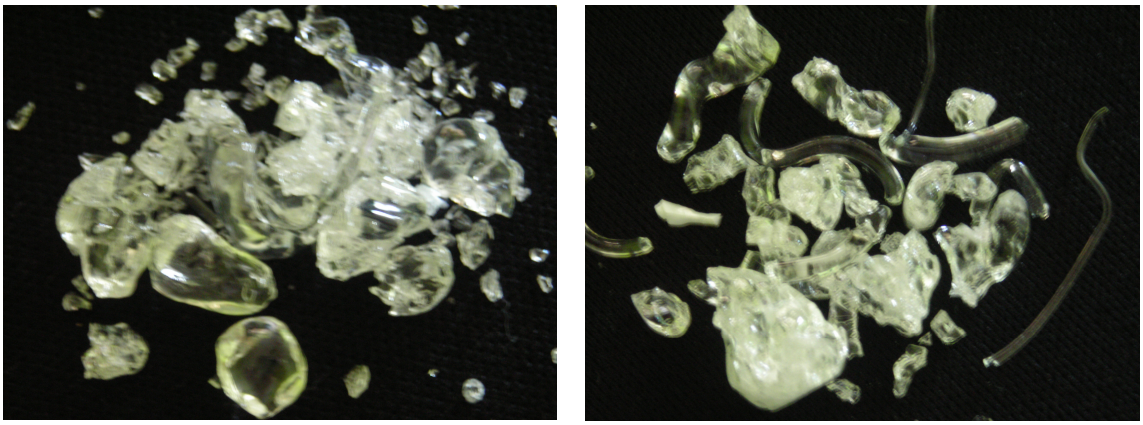

(a) transparent frit (b) opaque frit

Figure 2.4.1. Frit (solid granules)

Variety of minerals is fused in a furnace and then the molten material is quenched rapidly. The constituents of the feed material changes depending on whether the frit is to be used as a ground coat or as a cover coat. The primary constituents of the raw material include silica, fluorspar, soda ash, borax, feldspar, zircon, aluminum oxide, lithium carbonate, magnesium carbonate, and titanium oxide for cover coats. In the case of ground coat, same compounds are included plus smaller amounts of metal oxides such as cobalt oxide, nickel oxide, copper oxide, and manganese oxide are present. In order to understand the nature of the glaze and its properties, amounts of the various oxide molecules making up the glaze must be described.

In a given formulation for a frit composition, each oxide present has a contribution to make the glaze. The role of the common oxides is summarized as follows: SiO_2 is the most important oxide, by itself only has the ability to form glass if enough temperature is given. It is added in many forms such as quartz, feldspar, or wollastonite into a glaze. It mostly acts as a glass former and controls thermal expansion. Na_2O is useful flux over a wide temperature range. It functions in glaze systems as one of the potent fluxes. But its very high coefficient of thermal expansion is a disadvantage as glazes with high soda content craze on many bodies. Also, glazes rich in soda content found to be very soft and soluble in acids. LiO_2 is the most active of alkali fluxes. Because of its high cost, it is only used in glaze systems in which it is truly

needed. K_2O is very similar to Na_2O. It improves the gloss of the glaze. Alkaline earth oxide materials such as CaO, SrO, and BaO as well as MgO are generally added as raw materials and more typically added in fritted form. Their use is advantagenous as they

act as powerful fluxes without having a major effect on the thermal expansion of the glaze. ZnO is another useful flux above 1000^{o}C in smaller amounts. And when used in small amounts, acts as a catalyst to improve the fusion of other oxides. On the other hand, when added in large amounts it promotes crystalline effects and matteness/softness in greater amounts. But too much of it may cause the defects on the surface. Also, the presence of ZnO has an extensive effect on the colouring of the glaze. Lead oxide is another powerful flux, but besides its many advantageous properties, its toxicity limits its use. Al_2O_3 contributes into the working properties of glaze. It is normally added as calcined alumina or alumina trihydrate. It increases the melt viscosity. Also in presence of B_2O_3 or alkaline earths, phase separation is retarded or crystallization is observed. However, zirconium silicate is the major opacifier used in ceramic glazes, ZrO_2 is also primarily used as an opacifying agent. Less than 0.5 wt. % additions improve the alkali resistance. Finally, B_2O_3 is both a glass former and melting oxide. Whereas poor glaze durability is inevitable with excessive boron oxide addition. (Eppler et al. 2000).

CHAPTER 3

CORROSION

The word corrosion comes from the Latin word ‘corrodere’, means ‘gnaw away’. The most well-known form of corrosion is the rusting of iron and steel. Similar processes occur in other metals as well as in non-metallic materials, such as plastic, concrete and ceramics. According to the definition the term ‘corrosion’ stands for a process which takes place via a physicochemical reaction between the material and its environment and causes changes in the properties of the material (Mattson 1989).

It is defined as the destruction or deterioration of a material because of reaction with its environment. Although, some insist that the definition should be restricted for metals, corrosion engineers often consider non-metallic materials (Fontana 1986).

3.1. Corrosion Types

If different causes of corrosion and their mechanisms are considered, several types of corrosion can be thought of and can be classified in many different ways. One method divides corrosion as wet and dry corrosion depending on the presence of any liquid. A common example for wet corrosion is the corrosion of steel by water while attack of steel by furnace gases is an example for dry corrosion. On the other hand it can be divided as low temperature corrosion and high temperature corrosion (Fontana 1986).

The type of attack (corrosion environment) and the resulting appearance of the material also designate the type of corrosion. Water, soil, atmosphere and dry gases are considered as corrosion environments. Each type of corrosion can be identified by visual observation and for the basis of classification appearance of the corroded material is taken into account. Some of the corrosion types are given below (Mattson 1989):

3.1.1. Uniform Corrosion (General Attack)

It is the most common form of corrosion that proceeds uniformly at about same rate over the entire surface or over a large area when the material is exposed to a corrosive environment (Figure 3.1.1.). It is normally characterized by a chemical or electrochemical reaction and the extent can be given as the weight loss per unit area or by the average penetration (average of the corrosion depth).

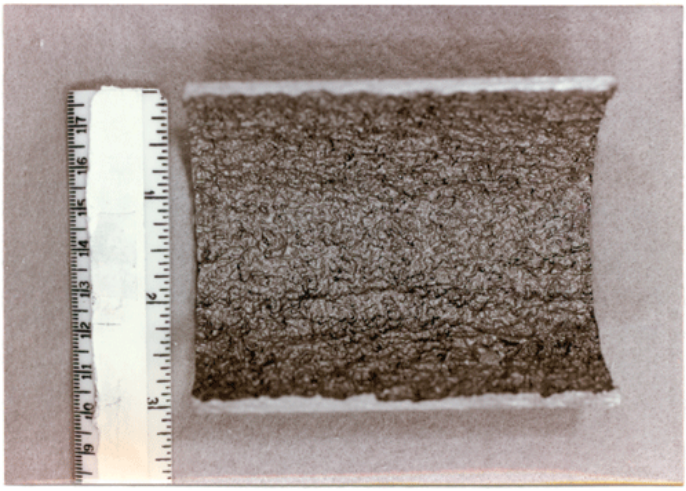

Figure 3.1.1. Uniform corrosion caused by CO_2.
(Source: WEB_2 2007)

3.1.2. Pitting

It is a localized corrosion which results in pits or in holes in the metal surface. The pits may have different diameter, but usually they are small in diameter and located in very close distance that the surface appears as a rough surface (Figure 3.1.2.). Pitting mostly results in worse damage than uniform corrosion, it causes equipment to fail because it can lead to perforation in a very short period of time. The number of the pits per unit area, the diameter of the pits and the depth of the pits should be taken into account in the evaluation of the attack.

Figure 3.1.2. Deep pitting in exchanger tubes.
(Source: WEB_3 2007)

3.1.3. Crevice Corrosion (Deposit or gasket corrosion)

Corrosion which takes place or immediately around the crevice is called, crevice corrosion (Figure 3.1.3.) . It is simply caused by the corrosive liquid being held in the crevice, while surrounding surfaces dry out or sometimes when the crevice and the surrounding metal surfaces are in a solution, the liquid in the crevice can be almost stagnant. This type of corrosion can take place in most metals and not only takes place in the crevices between surfaces of the same metal, but also when the metal is touching a non-metallic corrosion.

Figure 3.1.3. Aerospace alloy (Ti6Al4V).
(Source: WEB_4 2007)

3.1.4. Deposit Corrosion

This type of corrosion is caused by the moisture being held in or under the deposit (Figure 3.1.4.) . As the movement of the water is poor, corrosive conditions can be created under the deposit in a similar way described in crevice corrosion. For example, deposit corrosion is found under the road-mud in the wheel arch of the car or under leaves which have collected in guttering. The result is that a corrosion cell is formed with the anode under the deposit and the cathode at, or just outside, the edge.

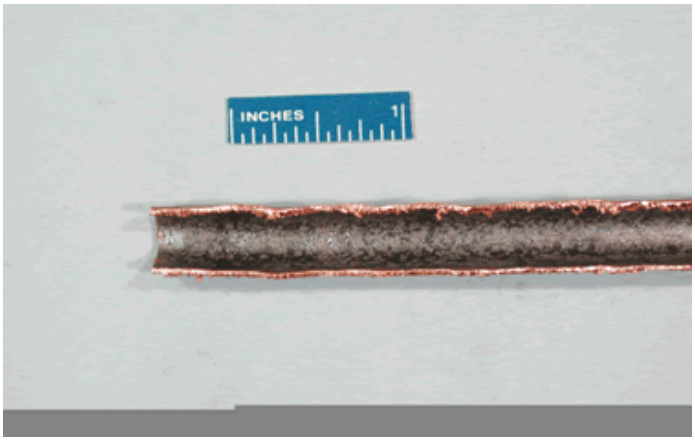

Figure 3.1.4. Deposit corrosion on the inside of bare.
copper sample, (Source: WEB_5 2007)

3.1.5. Selective Corrosion

The removal of the one element from a solid alloy at different corrosion rates can be named as selective corrosion (Figure 3.1.5.) . The most well-known example for selective corrosion is the dezincification of brass. As common yellow brass consists of approximately 30% zinc and 70% copper, on dezincification the zinc is selectively dissolved and copper is left as a porous mass having poor structural strength. Other similar corroison processes are the dealuminization and graphitic corrosion.

Figure 3.1.5. Selective removal of portions of a randomly generated plasma field.
(Source: WEB_6 2007)

3.1.6. Intergranular Corrosion

Metals are usually built of crystal grains and grain boundries are formed when a metal is solidifies or is heattreated. And this corrosion proceeds in or adjacent to grain boundries of the metal (Figure 3.1.6.). So, grain boundry region is caused to take on other corrosion characteristics that the main mass of the grain. Most well-known intergranular corrosion is in stainless steel. When the carbon concentration is too high in the precence of an unfavourable heat treatment chromium carbide formation occurs.

Figure 3.1.6. Rusted metal bolt
(Source: WEB_7 2007)

3.1.7.Layer Corrosion

In layer corrosion, the attack is localized to internal layers in wrought metal. This corrosion type is rather unusual and best known among the certain aluminun alloys. As a rule the layer is parallel to the direction of processing and to the surface. Formation of blisters those swelling the metal surface are observed.

3.1.8. Erosion Corrosion

All types of equipment exposed to moving fluids are subject to erosion corrosion. Because of a relative movement between corrosive fluid and metal surface, an acceleration in rate of deterioration is observed (Figure 3.1.7.). It involves conjoint erosion and corrosion. The attack is dependent on the degree of turbulance. Copper-bearing materials are particularly sensitive. As a result of this corrosion, pits with shiny surfaces free from corrosion products are formed in the direction of flow. Abrasive particles and air bubbles in the liquid increase the risk and intensity of erosion corrosion.

Figure 3.1.7. Water supply system
(Source: WEB_ 8 2007)

3.1.9. Cavitation Corrosion

A special form of erosion corrosion is cavitation corrosion. It occurs on surfaces where high-velocity liquid flow and pressure changes are encountered. Its appearance is similar to pitting, but the pits are not closely spaced and so the surface is not considerably roughened (Figure 3.1.8.). Cavitation corrosion can occur, in rotary pumps, on cylinder liners in engines and on ships' propellers.

Figure 3.1.8. Cavitation corrosion of deaerator
(Source: WEB_9 2007)

3.1.10. Fretting Corrosion

This type of corrosion describs the corrosion occuring at contact areas between materials under load subjected to slip and vibration. For fretting corrosion of metals in air, two considerations may be made: when two metal surfaces glide over eachother under pressure, small particles are released with continuous movement and they oxidize as a result of contact with oxygen in atmosphere and form finely divided, dark oxide powder (Figure 3.1.9.). On the other hand, as metal surface forms an invisible layer of oxide coating preventing further oxidation, at the contact points where the metal surfaces glide, a continous removal and rebuilt of the oxide is inevitable. So, this removed oxide forms discolour the points of contact.

Figure 3.1.9. Fretting corrosion of a fence post and wires.
(Source: WEB_10 2007)

3.1.11. Stress Corrosion Cracking (SCC)

Stress corrosion cracking (SCC) occurs in the presence of simultaneous tensile stress and a specific corrosive medium. It is only mechanical tensile stresses above a certain level which give rise to stress corrosion cracking while the corrosive media specific to the metal concerned, for example ammonia for copper alloys, chloride solution for austenitic stainless steel and nitrate solutions for copper alloys. The process of SCC, includes two stages, initiation and propagation. Initiation stage occurs before any crack becomes visible while propagation implies the growth of crack perhaps results in cracking (Figure 3.1.10).

Figure 3.1.10. Stress Corrosion Cracking on Mixer Bearing Support - (CSCC) Chloride Stress Corrosion Cracking, (Source: WEB_11 2007)

In the corrosion of non-metallic materials, for example in this study, ceramic materials, mechanisms like, dissolution of a refractory in contact with a liquid, any reactions which takes place in vapor, liquid and solid phases, penetration of the vapor or liquid phase into the pores, resulting in an altered zone are considered for the definition of corrosion (Nishikawa 1984). Type of corrosion in which the solid refractory is corroded by a molten glass is called dissolution. In order to find out the significance of refractory effect on the melt chemistry, dissolution studies should focus on the interface between refractory wall and the melt. Dissolution phenomenon can be classified into two, first known as the direct dissolution (also termed as congruent/homogeneous) involves the direct solution of the refractory species into the glass phase. In the case of selective dissolving of one or more phases, then it is called indirect (also termed as incongruent/heterogeneous). In case of indirect dissolution, a crystalline interface is formed as corrosion and/or dissolution is an interfacial process, meaning that developing due to the contact of species (Pecoraro et al. 1996).

Akira Nishikawa summarizes the corrosion phenomenon as follows:

A concentration gradient in refractory composition occurs when a refractory comes into contact with molten slag and dissolves. A boundary layer (interfacial film or diffusion layer) forms along the refractory wall. Components of the refractory specie, are diffused through this layer and dissolved into the liquid. At the same period, boundary layer and/or interfacial film resists to diffusion. This influence creates a contribution to the dissolution rate, and is called *the solution rate controlled by diffusion*, which is expressed by equation (3.1). :

$$dn / dt = DA/ \delta (n_s - n) \qquad (3.1)$$

n: concentration of the solute in liquid

n_s: saturation concentration of the solid

D: diffusion coefficient of liquid

A: contact surface area

δ: thickness of the interfacial film

t: time

The above formulation summarizes that the larger the concentration gradient, the faster the rate of dissolution, while thinner the interfacial layer and/or diffusion film, refractory dissolves more readily. On the other hand, viscosity of the slag also have an effect on the thickness of the interfacial film. Presence of different oxide constituents has a significant effect on the viscosity of the slag. In general, viscosity of slag increases, when the SiO_2 concentration increases. If the basic components are in large portions, viscosity of the slag is low. Apart from the composition of the slag, the below relation, equation (3.2). points out the effect of temperature on the viscosity of the slag that higher temperature results in a decrease in viscosity while an increase in dissolution rate, given as follows:

$$\eta = A \exp(-E/RT) \tag{3.2}$$

η : viscosity coefficient

A: constant

E: activation energy of a viscous flow

R: gas constant

T: absolute temperature

The second mechanism involved in corrosion, is the reaction corrosion of refractories occurring between, solid-solid, solid-liquid or solid-vapour phases. The control of the rate of reaction in solid phase reaction is related with the chemical reaction takes place at the boundary with respect to Fick's law or Jander's equation for reaction rate.

Corrosion of refractories mostly depend on the formation of a liquid phase. In this case, control of the rate of reaction is affected by following factors,

- Equation (3.3) defines the diffusion in the reaction layer ,

$$\alpha = kt \tag{3.3}$$

α : rate of reaction

t: time

- chemical reaction between the refractory and reaction layer given in equation (3.4),

$$1\text{-}3\ (1-\alpha)^{2/3} + 2\ \alpha = kt \qquad (3.4)$$

- diffusion in interfacial film.

The change in corrosion process with various conditions is defined by so many equations points out that very complex factors are governing this phenomenon.

The third mechanism considers the corrosion due to penetration: as pores exist in a refractory structure, liquids feel free to penetrate into refractory through the open pores those in contact with liquid. Capillarity is responsible for the main driving force for penetration. If the rate of corrosion proceeds due to penetration compared with the rate of dissolution or reaction corrosion, it is concluded that it develops at much faster rate as molten slag penetrates into relatively greater depths within the refractory resulting in a thick penetrated zone. The suction force in capillarity is mostly related with the surface tension (surface energy) and contact angle of liquid and refractory expressed as follows in equation (3.5).

$$\Delta P = 2\ \gamma_L \cos\theta / r \qquad (3.5)$$

ΔP : - suction force

γ_L : surface tension of liquid

θ : contact angle

r : capillarity radius

According to Jurin's theorem, equation (3.6) expresses the penetration depth as follows:

$$l = 2\ \gamma_L \cos\theta / r\rho g \qquad (3.6)$$

l : depth of penetration

ρ : density of liquid

g : accelaration due to gravity

Hagen- Poiesuille's equation expresses rate of penetration as follows,

$$l^2 = (\gamma_L r \cos \theta / 2 \eta) t \quad (3.7)$$

η : viscosity of liquid

t : time

$$\text{If,} \qquad k = \gamma_L r \cos \theta / 2 \eta \quad (3.8)$$

k: coefficient of penetration

$$l^2 = kt \quad (3.9)$$

Then, Zagar suggested that corrosion due to penetration depends also on the porosity and the relation is given in equation in (3.10). :

$$\frac{V}{\eta} = A (1/2 P^2 r \gamma_L t)^{1/2} \quad (3.10)$$

V : volume of penetrated liquid

A : area of the penetrated surface

P : apparent porosity

r : average radius of pores

The contact angle is the angle between the solid surface and the tangent to the liquid surface at the point of contact. It depends on the specific energies of the solid/vapor (γ_{SV}), solid/ liquid (γ_{SL}), and liquid/vapor (γ_{LV}) interface specific energies. The condition for the equilibrium of them is given in equation (3.11).,

$$\gamma_{SL} + \gamma_{LV} \cos \theta = \gamma_{SV} \quad (3.11)$$

Figure 3.1.11. summarizes the relation between the contact angle and penetration in solid-liquid-vapor phases. If $\gamma_{SV} > \gamma_{SL,}$ $\theta < 90^{o}$, the liquid phase wets the solid phase, and if $\gamma_{SV} < \gamma_{SL}$, then $\theta > 90$, it does not.

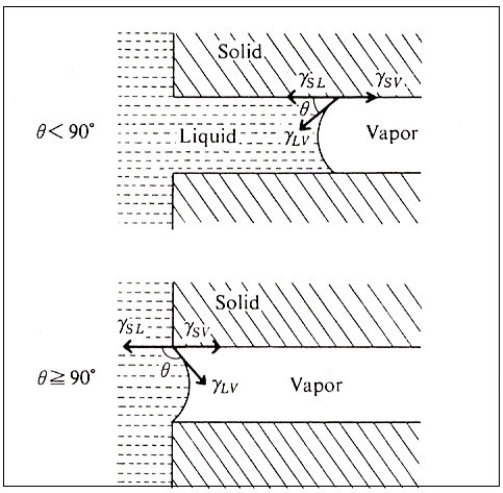

Figure 3.1.11. Contact angle via penetration.
(Source: Akira Nishikawa 1984)

If the above given relation is adjusted due to the penetration of liquid phase between neighbouring refractory grains, it is expressed in equation 3.12. as follows:

$$\gamma_{SS} = 2\,\gamma_{SL} \cos \theta / 2 \qquad (3.12)$$

If $\gamma_{SS} < 2\gamma_{SL}$, $\theta > 0$, (Figure 3.1.12.), the liquid phase can not penetrate. However, $\gamma_{SS} > 2\gamma_{SL}$, the liquid penetrates between the grains.

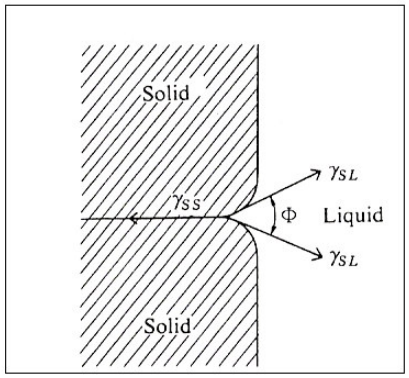

Figure 3.1.12. Contact angle via penetration in solid-liquid phases.
(Source: Akira Nishikawa 1984)

To sum up, surface energy of the refractory material, surface tension of the molten slag and the interfacial energy between the solid and the liquid are said to be the factors responsible for penetration. And the degree of penetration mostly affected by the composition of the slag.

3.2. Corrosion Resistance of Refractories to Molten Process Liquid (Slag)

Molten liquid responsible for corrosion may vary depending on the industrial application of the refractory. Aksel, studied the corrosion of alumina-mullite-zirconia refractories those used in glass industry, by standard soda-lime-silicate glass and concluded that solubility of alumina was much higher than zirconia, that needle-like alumina crystals were observed, while zirconia particles made an effective barrier (Figure 3.2.1.a.), (Aksel 2003).

Fredderici et al. have studied the corrosion of Al_2O_3-ZrO_2-SiO_2 (AZS) and Al_2O_3-ZrO_2 (AZ) by a mixture of blast-furnace slag and cullet (soda-lime glass) and found no difference between the corrosion resistance of the two materials with a homogeneous observation of alumina and mullite at the interface (Fredderici et al. 2000).

On the other hand, Leigh et al., tested high-alumina crucible for the corrosion behaviour of three types of steelmaking slags on MgO-C ladle refractories, and stated that the degree of slag attack was related to the carbon loss (Figure 3.2.1.b.), (Leigh et al. 1987).

Santos et al., conducted corrosion tests in which heavy metal oxide glass was used as a process liquid. Depending on their chemically corrosive nature and dissolving behaviour during melting step in different degrees, almost all the well-known refractories used in making crucibles, and also gold and platinum were damaged (Santos et al. 2003).

Dunkl et al., points out that in the case of a typical virgin fused cast Al_2O_3-ZrO_2-SiO_2 (AZS) structure corroded by soda-lime glass, the resulting microstructure has large alumina crystals and their co-precipitated zirconia, zirconia dendrites and the glassy phase (Dunkl et al. 2003).

Lee et al., studied the bottom drilling corrosion in electrocast Al_2O_3-ZrO_2-SiO_2 (AZS) refractories, and reported the examination of the microstructure developed around a metal droplet where a continous aluminosilicate glass matrix surrounding pure

ZrO_2 dentrites and corundum heterogeneous grains made up of pure corundum with the Al_2O_3-ZrO_2 eutectic (Lee et al. 1996).

The influence of liquid phase on the slag corrosion of andalusite-based refractories was studied at 1600°C using the crucible method by Poirier et al., like in all static crucible tests, four textures were formed: (1) unaffected refractory (2) penetrated zone (3) precipitation zone (4) remaining-slag zone. This penetrated zone and/or the precipitation zone make up the interface under study and the resistance to slag corrosion of andalusite based refractories was observed to be governed by the evolution of the liquid-slag composition at service temperature: as the content of SiO_2 increases, the dissolution rate of mullite decreases (Figure 3.2.1.c.), (Poirier et al. 2004).

Manfredo et al., tested the corrosion of fusion-cast high zirconia Al_2O_3-ZrO_2-SiO_2 compositions against soda-lime glass. And the result pointed out that this material showed no improvement over the corrosion resistance of a typical commercial AZS refractory containing 40 wt. % ZrO_2 (Figure 3.2.1.d.), (Manfredo et al. 1984).

Increased corrosion resistance of alumina-zirconia-silica (AZS) refractories used in glass melting furnaces is a fact by the interlocking of alumina crystals and the glassy matrix by ZrO_2 dentrites. However, Asokan has studied the variation in the microstructure of AZS upon heat treatment and observed the significant dimensional changes (Asokan 1994).

Dissolution of two different alumina types (commercial white fused and tubular) into silicate melt was investigated by Zhang et al. Formation of CA_6 and hercynitic spinel layers was obvious at all Al_2O_3-melt interface (Zhang et al. 2006).

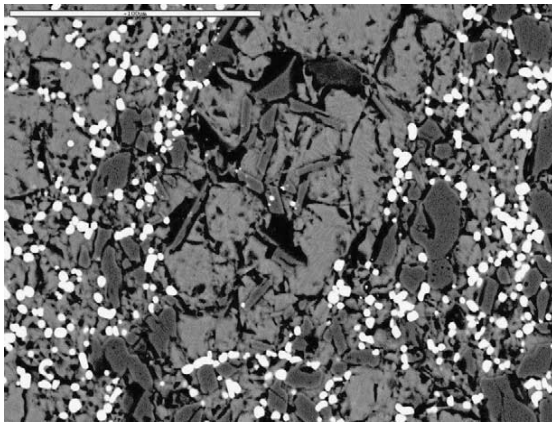

(a) Cemail Aksel 2003, microstructure of Alumina-Mullite-Zirconia bricks, showing the initiation of glass penetration in Zone I (scale bar: 100 mm).

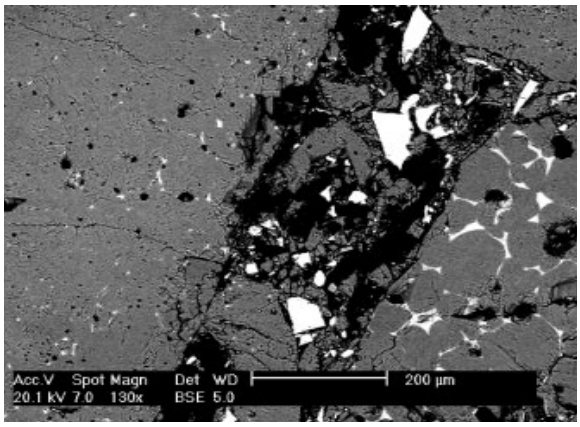

(b) Leigh et al. 1987, bottom right periclase grain is a low-quality sinter with a high proportion of low-melting intergranular bond phase. Angular silicon and rounded aluminum particles

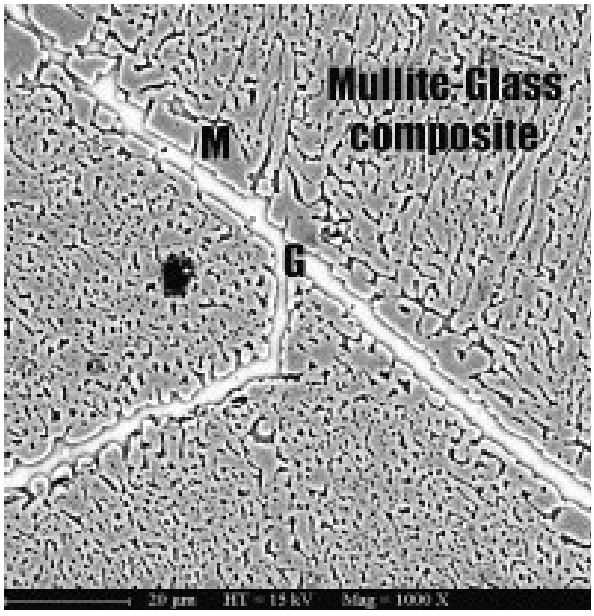

(c) Poirier et al. 2004, original brick showing the mullite-glass composite

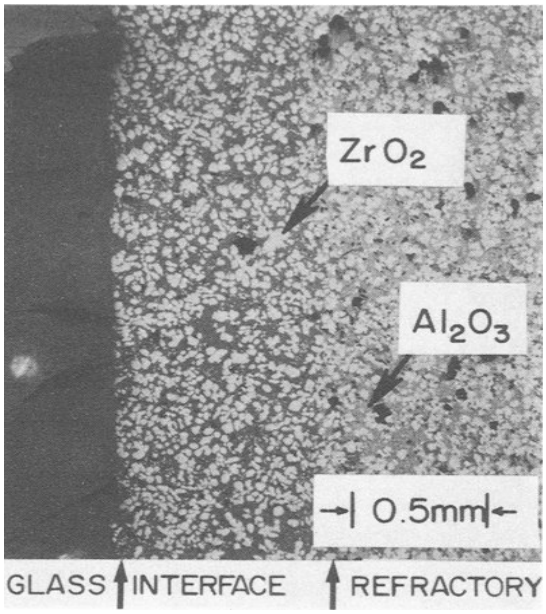

(d) Manfredo et al. 1984, corrosion interface between soda lime glass and a typcial commercial $A1_20_3$-ZrO_2-SiO_2 fusion-cast refractory.

Figure 3.2.1. SEM micrographs of corroded zones and phases formed

3.3. Phase Diagrams

Phase diagrams can reduce the need for expensive and time consuming experiments. The compatibility between refractories and liquids indicates the corrosion resistance of different refractories and assist the selection of the proper refractories for specific applications. Phase diagrams can be used to consider the design of refractories composition. Therefore, the corrosion of high temperature refractories and other ceramics can be evaluated by the information available in existing phase diagrams (WEB_11 2007).

Morelli et al., used Al_2O_3-ZrO_2-SiO_2 ternary phase diagram in order to study the corrosion resistance of AZS and AZ crucibles against a glass prepared from a blast-furnace slag and cullet (Morelli et al. 2000). The mentioned phase diagram showed that in both compositions the phases in equilibrium were the same and that the first liquid formed at about 1380 ^oC might have been responsible for the corrosive process, considering that this temperature was very close to the working temperature.

Lecomte et al., experimented the thermal transformations of compounds belonging to two vertical sections between mullite and the eutectic point at 985 ^oC or the peritectic at 1140 ^oC in Al_2O_3–K_2O–SiO_2 system. In both sections, results indicate the particular shape of liquidus curves, which show accentuated slopes at the vicinity of eutectic and peritectic points (Lecomte et al. 2004).

One can determine the type of dissolution and formed interface constituents, by examining the phase diagram related to that system. Osborn et al., studied the CaO-Al_2O_3-SiO_2 system to mark a selected glass composition at the eutectic 1265 ^oC, and was in contact with alumina at 1500 ^oC. The dissolution was observed to be indirect and the interface was determined to consist of $CaAl_{12}O_{19}$ (Osborn et al. 1960).

Manfredo et al., also used Al_2O_3-ZrO_2-SiO_2 ternary system in order to test the corrosion resistance of nine compositions of prepared glass batches to soda-lime glass. Compositions one to nine on the AZS ternary system constituted an experimental design that contains the different zirconia volume percent estimations with varying molar ratio of Al_2O_3 to SiO_2 (Manfredo et al. 1984).

In order to understand the compatibility of transparent and/or opaque frit composition, with the possible refractory materials, ternary phase systems, Al_2O_3-K_2O-SiO_2 (AKS) and Al_2O_3-ZnO-SiO_2 (AZS) were used. These diagrams were given in

Figure 3.3.1. (Schairer 1947) and Figure 3.3.2. (Bunting 1932), respectively. Four major constituents in each transparent and/or opaque frit over the total weight percent were calculated as follows, for transparent frit composition, the compositions consisting of, potassium oxide (K_2O) 9 wt. %, alumina (Al_2O_3) 13.6 wt. % and silica (SiO_2) 77.4 wt. % on AKS ternary system, while zinc oxide (ZnO) 17.11 wt. %, alumina (Al_2O_3) 12.43 wt. % and silica (SiO_2) 70.45 wt. % on AZS system were determined. In the case of opaque frit, in AKS system, potassium oxide (K_2O) 8.26 wt. % , alumina (Al_2O_3) 6.9 wt. % and silica (SiO_2) 84.8 wt. %, while zinc oxide (ZnO) 16.2 wt. %, alumina (Al_2O_3) 6.3 wt. % and silica (SiO_2) 77.5 wt. % in AZS system were calculated, respectively. The important crystal phases of AKS ternary system were observed to be, potash feldspar ($K_2O.Al_2O_3.6SiO_2$), leucite ($K_2O.Al_2O_3.4SiO_2$), mullite ($3Al_2O_3.2SiO_2$), potassium silicates, and SiO_2 modifications. Both the calculated transparent and/or opaque frit compositions lie in the field of mullite region. When a straight line is drawn from the point of composition to the crucible material (Al_2O_3), presence of any liquidus curve that might form low-melting eutectics was not observed for both compositions.

On the other hand, in Al_2O_3-ZnO-SiO_2 system, crystallization of $ZnAl_2O_4$ was observed at 1950 ^oC. In both frit melt- alumina crucible wall interface, this crystal structure was formed, which will be mentioned in detail in Chapter 5. However, the frit melting temperature was 1500 ^oC, the presence of other fluxes might reduce the $ZnAl_2O_4$ formation temperature indicated at the AZS ternary phase diagram. So, study of AZS phase diagram resulted in aggrement with the characterization methods in the case of observing the formation of $ZnAl_2O_4$ crystals. Zirconia on the other hand dissolved from the frit composition and reprecipitated during cooling. Clusters and chains of small spherical ZrO_2 grains grew with a dentritic shape mainly adjacent to the interface formed in opaque frit-alumina crucible wall. As, zirconia is a well-known nucleating agent for crystallization in glasses, the small crystals of zirconia which precipitated in the opaque frit interface promoted the crystallization of $ZrSiO_4$ in opaque frit matrix.

In order to understand the behaviour of ZrO_2 against frit compositions, Al_2O_3-ZrO_2-SiO_2 (Figure 3.3.3.) ternary system was studied, as Barbieri et al., state that the phase diagram of the system K_2O-ZrO_2-SiO_2 has not yet been reported in literature depending on the diffuculty in adaption of the high melting points of ZrO_2 and SiO_2 with the high volatility of K_2O (Barbieri et al. 2002). Binary phase diagram of ZrO_2–SiO_2 is given in Figure 3.3.4. The compositions indicating the calculated percentages of

SiO_2 present in both transparent and/or opaque frit lie in the $ZrSiO_4$+SiO_2 region where no liquid was observed to be responsible for corrosion. However, the individual phase diagram of ZrO_2, points out the phase transformations (Figure 3.3.5). The solid zirconium oxide, ZrO_2, has three modifications. The low-temperature phase, m-ZrO_2, has monoclinic crystal symmetry. The intermediate-temperature phase, t-ZrO_2, is tetragonal, while the high temperature ZrO_2 has cubic structure (Chen et al. 2004). In this study, in the frit melting temperature of about 1400-1500 ^{o}C, monoclinic to tetragonal transition occurs upon heating schedule causing extraction and/or contraction mismatches during cooling cycle.

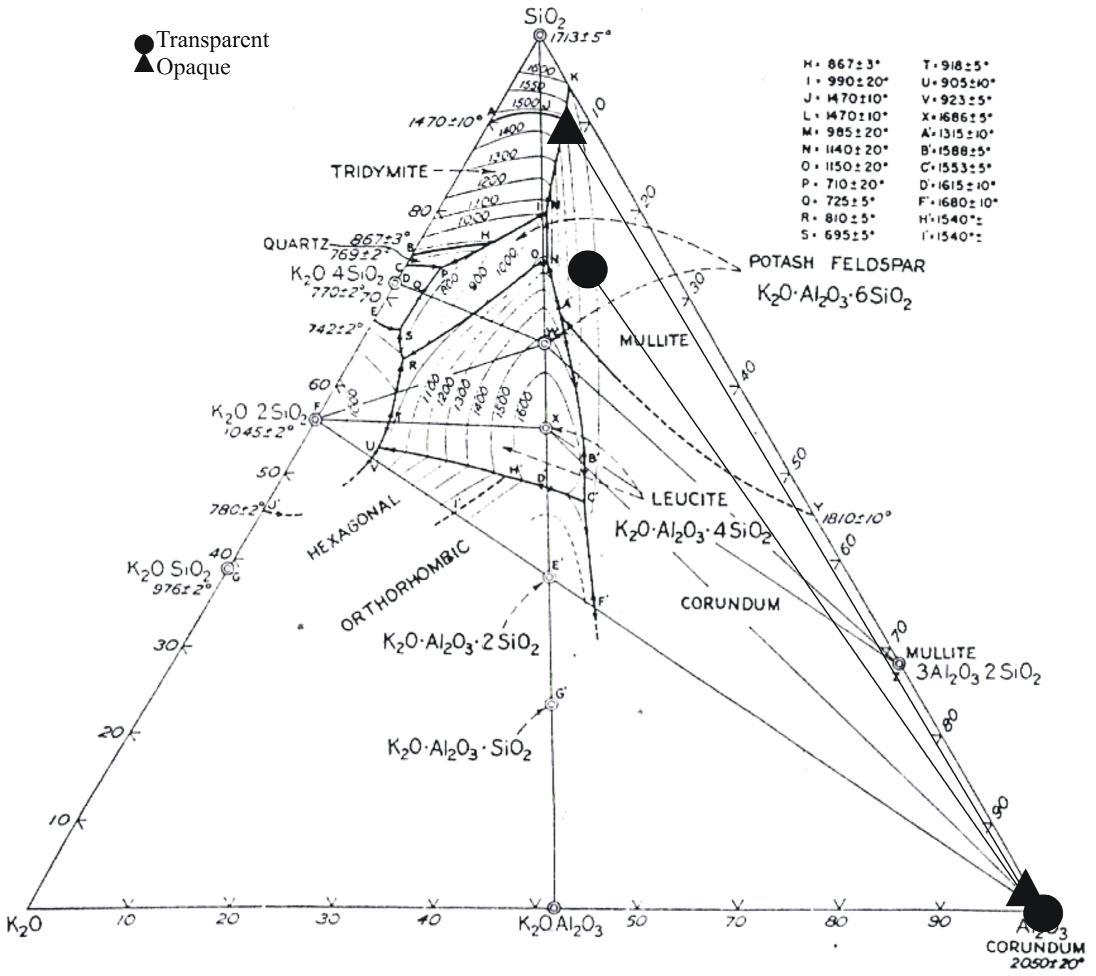

Figure 3.3.1. Al_2O_3-SiO_2-K_2O ternary system. Composition of the frit is indicated in terms of the major components shown on the diagram (Source: Schairer 1947).

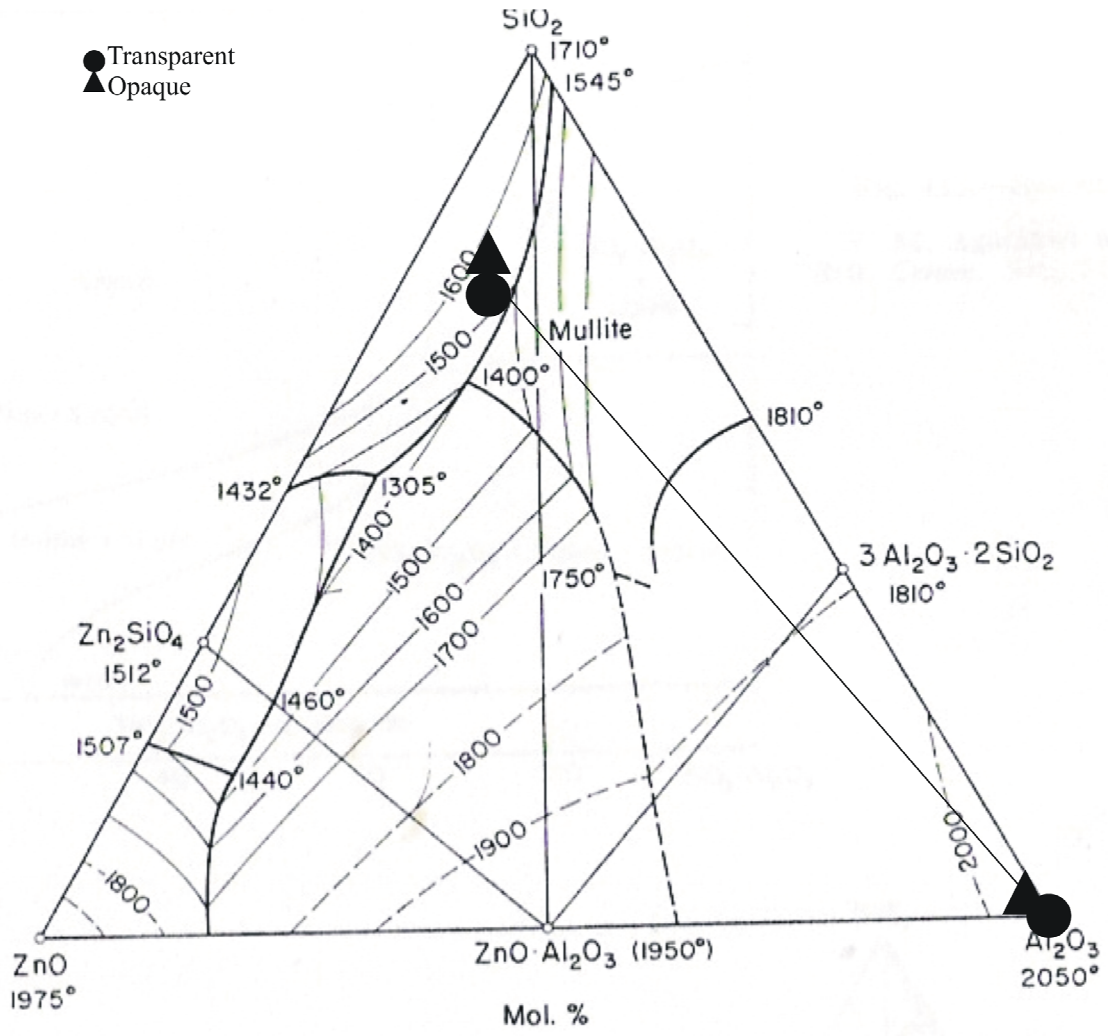

Figure 3.3.2. Al_2O_3-SiO_2-ZnO ternary system. Composition of the frit is indicated in terms of the major components shown on the diagram (Source: Bunting 1932).

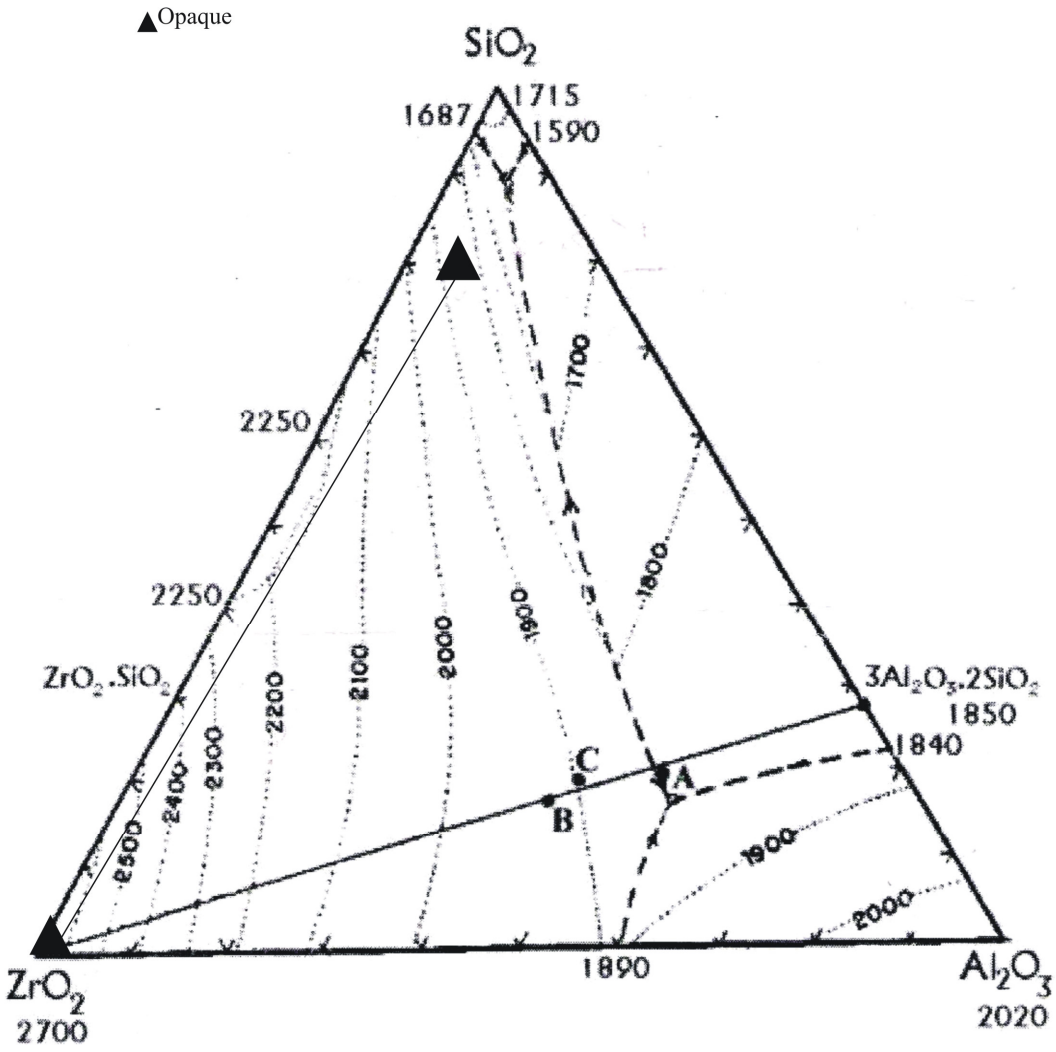

Figure 3.3.3. Al_2O_3-SiO_2-ZrO_2 ternary system

(Source: Fredericci et al. 2000)

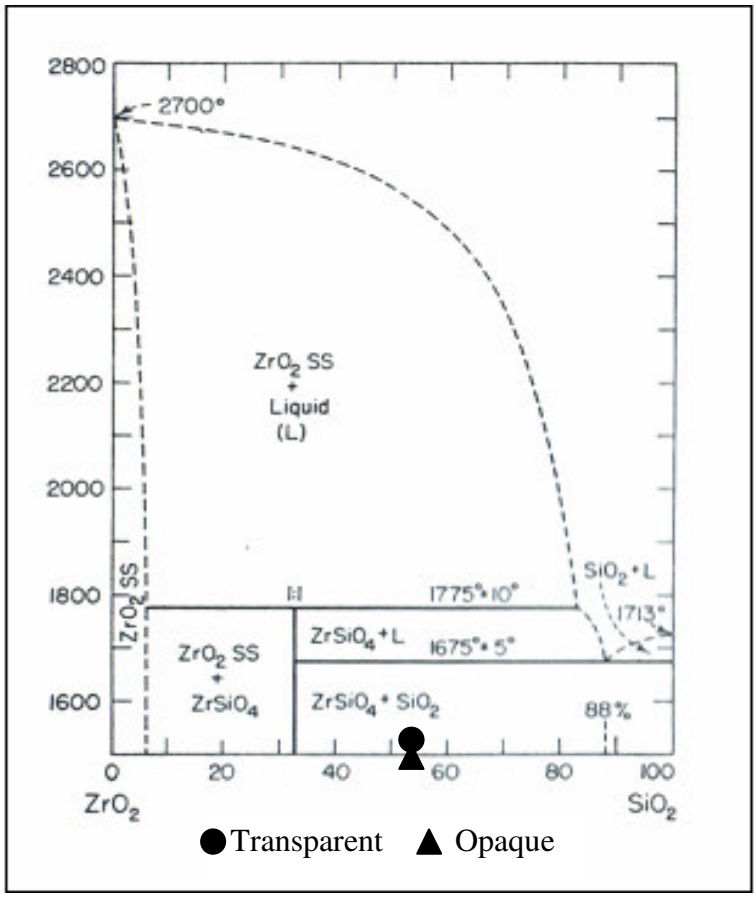

Figure 3.3.4. ZrO_2-SiO_2 binary system.

(Source:Phase Diagrams for Ceramists 1956)

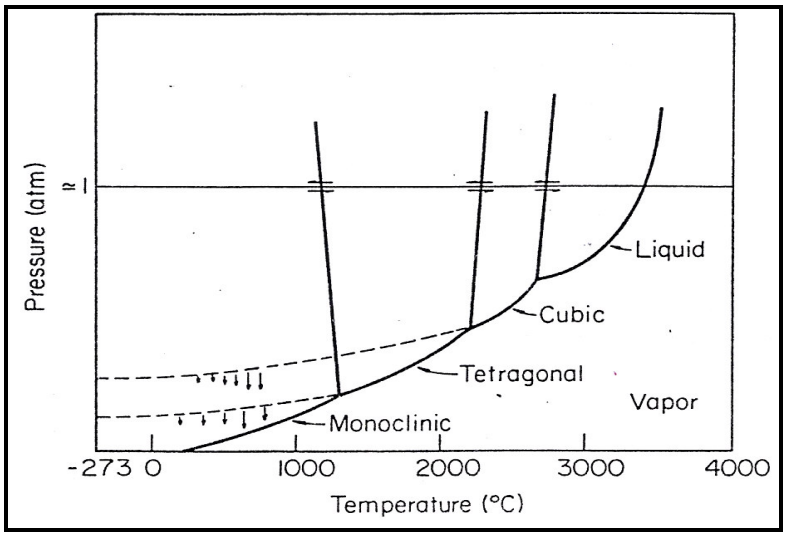

Figure 3.3.5. ZrO_2 system.

(Source: Ruh and Rockett 1970)

CHAPTER 4

EXPERIMENTAL

In this chapter the production of crucibles from powder raw materials, the characterization of frit and the corrosion tests are presented. In the first section, the properties of the crucible materials, alumina (A), zirconia (Z) and alumina-zirconia (AZ) from powder to sintered ceramic articles are given. The two frit species, mainly transparent and opaque frits and their characteristics are also shown. Finally, the high temperature treatment of crucibles and frit melt for study of corrosion are explained.

4.1. Crucibles and Frits

In this study, two types of frits were used for corrosion testing of the crucible materials (Tamsa Seramik, İzmir-Türkiye). Their chemical composition was given in Table 4.1.1. The first frit was opaque frit containing zircon and the second one was a transparent frit without the zircon but with higher zinc and aluminum. These were commercially used frits that are applied on wall and floor tile glazes. Thermal expansion behavior of the frits were analyzed by a horizontal dilatometer (Linseis, Germany).

In this study, three different types of crucible materials were tested and investigated. As mentioned earlier, the selection of the crucible material was based on the use of three component phase diagrams that most closely covered the composition of the frit and the crucible. The materials to be potentially used for making crucibles were identified as Al_2O_3 and ZrO_2. The powder raw materials were determined with respect to their availability and cost. Commercial alumina powder (Alcoa CT–3000 SG) was obtained from Alcoa Industrial Chemicals, Germany and zirconia (TZ-3YE) from TOSOH, Japan having particle sizes of 0.7 µm, specific surface area (BET) 7.0 m^2/g and 0.5 µm, specific surface area (BET) 16 ± 3 m^2/g, respectively.

Table 4.1.1. Frit Compositions

	Transparent frit wt%	**Opaque frit wt%**
Al_2O_3	9.3	4.1
B_2O_3	8.5	7.6
BaO	0.0	1.8
CaO	8.4	12.1
K_2O	6.1	4.9
MgO	2.2	0.0
Na_2O	0.0	0.0
SiO_2	52.7	50.3
ZnO	12.8	10.5
ZrO_2	0.0	8.7

Slip-casting method was used for the production of crucibles. In this method as indicated in the previous chapters, preparation of a stable suspension was a primary requirement. So, identifiying the nature of the suspension in other words, a rheological study was necessary, hence control of the dispersion was critical. Ranges of shear rate encountered in ceramic processing operations are indicated in Figure 4.1.1. (Reed 1995). The slip to be used in casting should satisfy the pouring behaviour, so depending on the given figure the shear rate is kept between 0.1 and 100 sec^{-1}, with analysis duration of 100 seconds and 101 data were taken. In order to see the effect of solids loading in the preparation of Al_2O_3 suspensions, viscosity measurements were conducted. Figure 4.1.2. pointed out that there was a direct correlation between the solids loading and viscosity of the system.

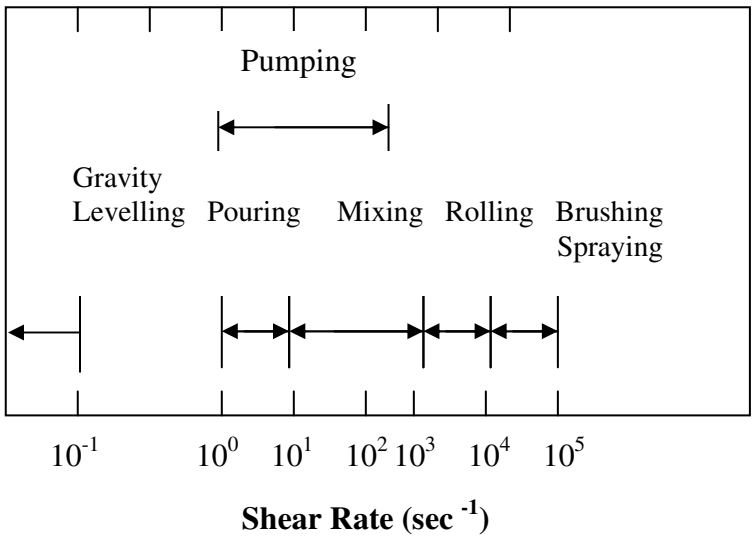

Figure 4.1.1. Different processing operations occurring in different ranges of shear rate. (Source: Reed 1995)

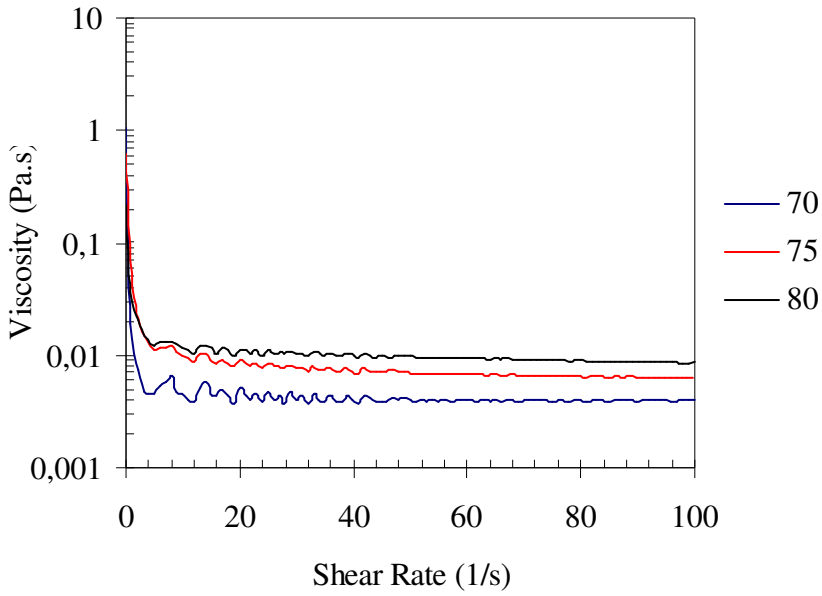

Figure 4.1.2. Al_2O_3 solids loading effect on viscosity

On the other hand, for the selection of the best deflocculant to be used in the preparation of ZrO_2 slip, six different commercially available deflocculants were tested by preparing mixtures via addition of 7.7 g of ZrO_2 (TOSOH-TZ-3YE) and 2.3 mL of water in a magnetic stirrer. Measurements of viscosity of different suspensions were done in a Haake Mars Modular Advanced Rheometer and the best combination of

deflocculants was identified. Added electrolytes and polymers may significantly change interparticle forces and the state of dispersion. Taylor et al., classify deflocculants in two types: the polyanion complex, salts of sodium and phosphoric acid such as sodium tripolyphosphate, tetrasodium pyrophosphate and sodium metaphosphate and the alkali cation deflocculants, monovalent salts such as sodium nitrite, borax, sodium aluminate, ammonium hydroxide and sodium carbonate or potassium carbonate (Taylor et al. 1986). In order to achieve stable suspensions, after a literature search, the most effective deflocculants for the stabilization of alumina and/or zirconia suspensions were determined as Darvan-C (Vanderbilt Co. Norwalk, CT, USA) and Dolapix CE–64 (Zschimmer&Schwartz Lahnstein /Germany), respectively. Both deflocculants develop steric and/or electrical stabilization in the suspensions. Darvan-C is the mixture of ammonium polymethacrylate and water whereas Dolapix CE–64 is a carbonic acid based synthetic polyelectrolyte. Polyelectrolytes have a double role of particle charging and electrosteric stabilisation of the suspension, (Popa et al. 2006). Their mechanism of deflocculation is much different than the inorganic salts. As they are made up of many carboxyl $-COO^-$, a high adsorption is observed due to electrostatic forces between positively charged particles and $–COO^-$ groups (Tsetsekou et al. 2001). When the water soluble part of the chain is dissolved in the media, the remaining hydrocarbon groups lay down on the particle surface, and the COO^- moieties remain as far from the particle surface as their branch lenght will allow (Dunk and Dinger 1993). The formed layer around each particle would create a repulsive force enabling the proper dispersion of the system. Whereas, addition of excess amount of the deflocculant and/or electrolyte may result in thixotropic behaviour of the suspension, in other words, high-solids coating slips exhibit thixotropy. An application process can be both eased and hurt by this property (Eppler et al. 2000).

Plaster is a useful material for use in ceramic forming molds due to its water absorption capability. After stable slips for each crucible materials were prepared, plaster molds were made by using water/plaster ratio of 1:1.4 (Figure 4.1.3.). Prepared slips were poured into plaster molds and when a desirable thickness has been reached the excess slip was poured back. Finally the body was removed out of the mold when the edges of the cone-shaped crucible were observed to be separated from the mold due to drying shrinkage.

Figure 4.1.3. Plaster Moulds.

The green bodies were initially dried at 110^{o}C for an hour in order to prevent thermal-shock and evaporate the excess water that might remain in the body. Finally, depending on the temperature at which the compacts reached high density, they were sintered at 1550 ^{o}C with a heating rate of 10 ^{o}C/min in a high-temperature box furnace (Nabertherm, Germany) for two hours. Archimedes' method was used in order to calculate the percent water absorption of the products and the results confirmed that the fired crucibles were found to be fully dense and impervious (Table 4.1.2). As can be seen from the data measured for each crucible sample, the products were found to be free of pores with a very little portion of water absorption.

Table 4.1.2. Density measurement of Al_2O_3 (A) and ZrO_2 (Z) crucible samples by Archimedes' Method.

Crucible Sample	Dry weight, D	Suspended weight, S	Saturated weight, W	Exterior vol., cm^3	vol of open pores, cm^3	vol of impervious portion, cm^3	Apperent Porosity, %	Water Absorption, %	Apperent Specific Gravity, gr/cm^3	Bulk Density, gr/cm^3	Theoretical Density, %
A1	1.53	1.14	1.53	0.39	0.00	0.39	0.79	0.20	3.93	3.90	98.5
A2	1.31	0.98	1.31	0.34	0.00	0.34	0.92	0.24	3.93	3.90	98.4
A3	0.81	0.60	0.81	0.20	0.00	0.20	0.78	0.20	3.94	3.91	98.8
Average A	1.21	0.91	1.22	0.31	0.00	0.31	0.83	0.21	3.94	3.90	98.6
Z1	3.05	2.54	3.05	0.52	0. 00	0.51	0.85	0.14	5.96	5.91	97.6
Z2	2.28	1.89	2.23	0.38	0.00	0.38	0.54	0.09	5.91	5.88	97.2
Z3	1.72	1.43	1.72	0.29	0.00	0.29	0.38	0.06	5.96	5.93	98.1
AverageZ	2.35	1.95	2.35	0.39	0.00	0.39	0.59	0.10	5.94	5.91	97.6

As both crucible species were obtained free of serious defects and were impervious, melting of frits within these crucibles was conducted. The melting of species was done between 1400 and 1500^{o}C with a heating rate of 10^{o}C/min for an hour of dwell time at target temperature. Crucibles were removed from the furnace after the frit melting experiment and sectioned using a diamond saw. As the main purpose of this study was to investigate the interface developed between the crucible material and the frit species, standard ceromographic grinding and polishing techniques were carried out on the glass-crucible wall interface.

4.2. Characterization Tools

The following characterization sequence is followed:

(i) Both alumina and zirconia powders were analysed by scanning electron microscopy (SEM) Philips XL-30S FEG equipped with EDS unit (EDAX).

(ii) The suspensions from each powder were prepared by addition of the proper amounts of required deflocculants. Agglomeration was prevented by well-balanced additions of the electrolytes. In order to obtain a stable agglomerate-free suspension, mechanical mixing was carried out as presence of any size of the particulate matter causes defects during sintering process.

(iii) Depending on the environmental factors such as the temperature and/or humidity of the room, the separation of green bodies from the molds varied. A superior care must be taken during and/or after the removal of the wet crucibles as green body form of the ceramics are known for their sensitivity.

(iv) Chemical interactions between the processing liquid (frit) and the crucible were investigated in this study by using an optical microscope (OM, Nikon Eclipse L150), and a scanning electron microscope (SEM, Philips XL-30S FEG) equipped with Energy Dispersive Spectroscopy (EDS) unit. X-ray diffraction (XRD, Philips X'Pert Pro) was used in order to confirm the crystalline phases formed at the interface. Frit-alumina, frit-zirconia and frit- alumina- zirconia mix samples representing the interface region were prepared for SEM-EDS, OM and XRD analysis by common ceramographic grinding and polishing techniques.

EDX analysis was conducted on the composition of the melted and original transparent and/or opaque frit in Al_2O_3 crucible in order to indicate any dissolution

occurs during melting processes. Comparison of the elemental compositions of both original transparent and/or opaque frit and melted (1500 ^{o}C) transparent and/or opaque frit is given in the following chapter.

Before conducting dilatometric measurements for the determination of thermal expansion coeffiecients of frit species, DTA and TGA analysis for both transparent and/or opaque frit were done to define T_g for both of the frit species, under nitrogen gas with a flow rate of 200 ml/min and a heating rate of 10 ^{o}C/min.

Dilatometric measurement was done by a horizontal dilatometer, Linseis, Germany, for the determination of the thermal expansion coefficient of frit species in order to comment on the extraction and/or expansion mismatch of them with the crucible materials.

CHAPTER 5

RESULTS AND DISCUSSION

In this chapter, microscopic, X-ray diffraction and thermal analysis investigations for materials used in the production of crucibles and for transparent and/or opaque frit are reported.

5.1. Characterization of Crucibles and Frit

Perfect circular geometry of the ZrO_2 granules and cancellous view of the Al_2O_3 powder were observed by SEM as given in Figure 5.1.1. respectively. Also, Figure 5.1.2. shows the published particle size distribution of alumina powder from which d_{50} is observed to be as 0.7 μm (Alcoa Industrial Chemicals 2007).

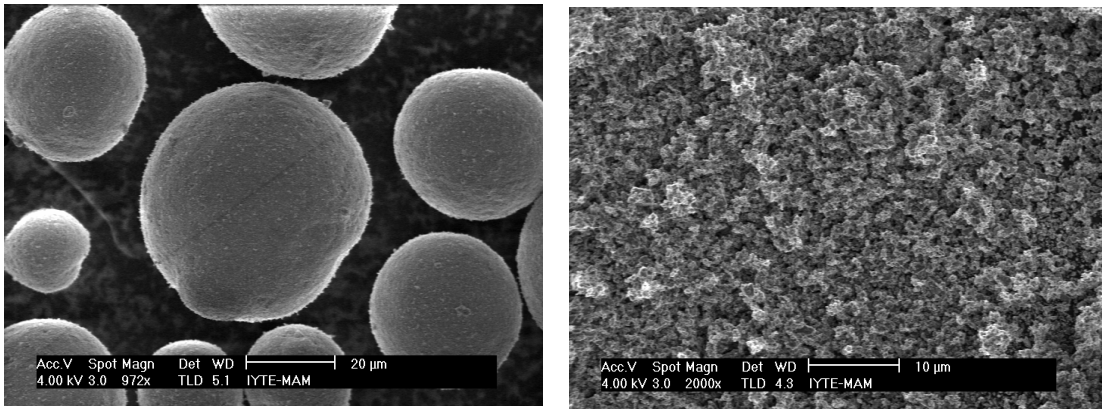

(a) ZrO_2 granuleTosoh TZ-3YE (b) Al_2O_3 powder Alcoa CT-3

Figure 5.1.1. SEM micrographs of the studied powders

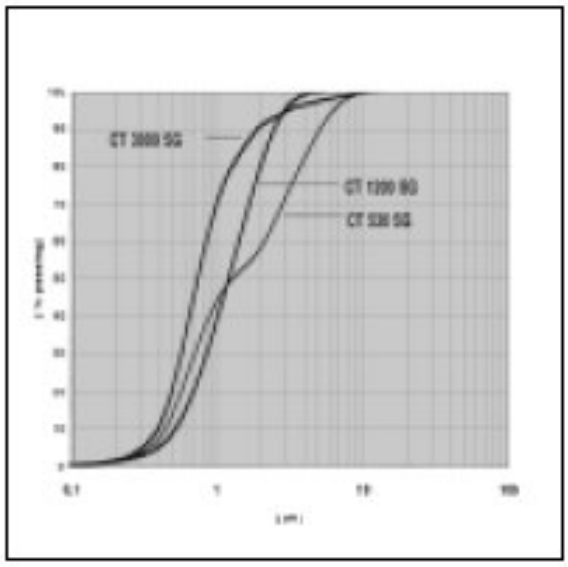

Figure 5.1.2. Particle size distribution of Al_2O_3.
(Source: Alcoa Product Data 2007)

The DTA/TGA analysis resulted in an increament in the weight percent of the species which might be explained by the sticking of the species on the surface of the crucible (Figures 5.1.3. and 5.1.4.).

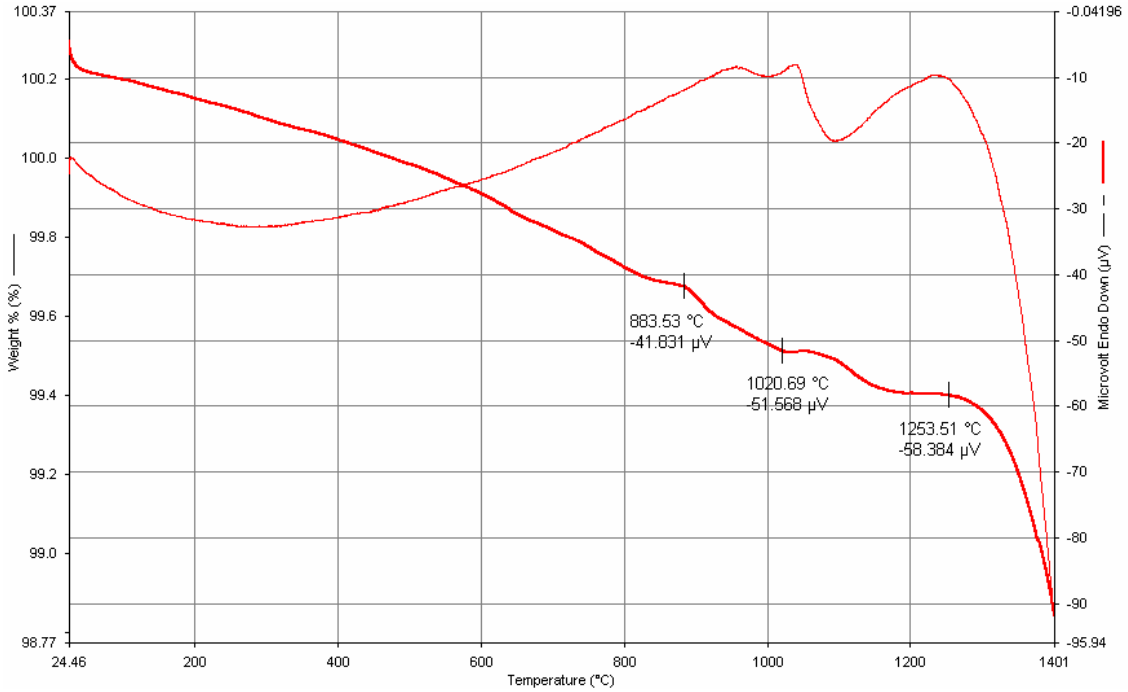

Figure 5.1.3. DTA/TGA analysis for transparent frit

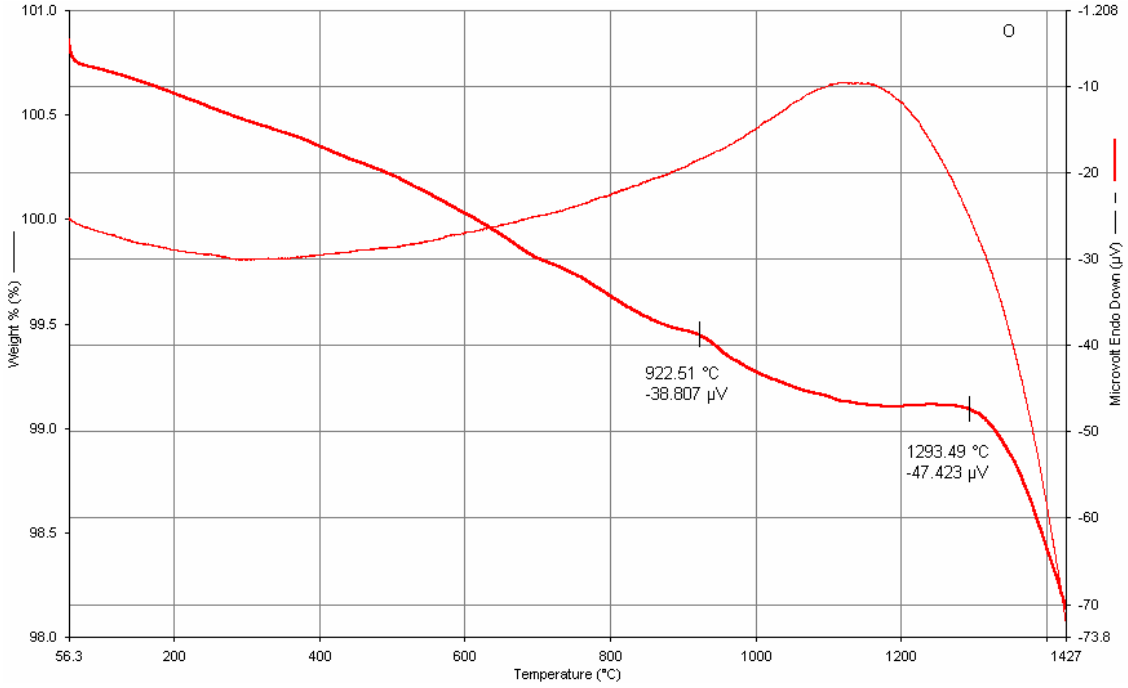

Figure 5.1.4. DTA/TGA analysis for opaque frit

The coefficient of thermal expansion (CTE), α, of frit species were determined by dilatometric analysis from the below T (^{o}C) vs ΔL plot Figure 5.1.5. The values calculated from the plot with respect to the equation 5.1, were found as 4.0 x 10^{-6}/ ^{0}C (150 ^{o}C) for transparent frit and 8.2 x 10^{-6}/ ^{0}C (150 ^{o}C) for opaque frit, respectively.

$$\text{Coefficient of linear thermal expansion} = CTE_L = \Delta L / (L_o \times \Delta T) \qquad (5.1)$$

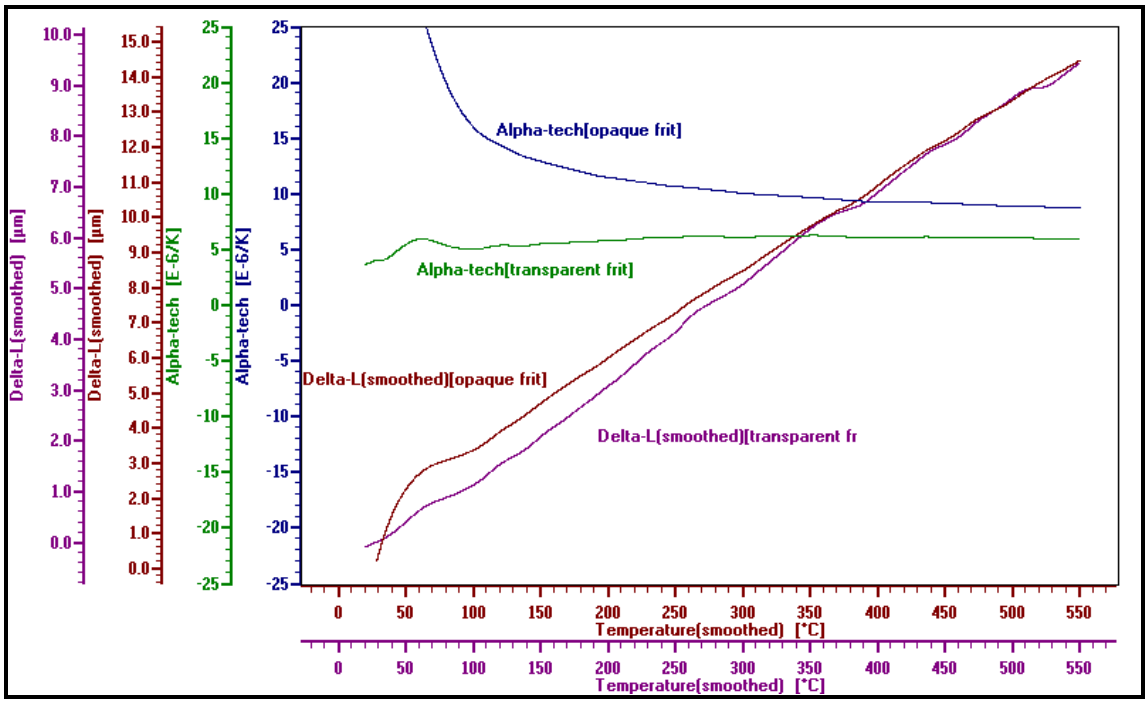

Figure 5.1.5. CTE determination by dilatometric measurement

Different methods for producing stable ceramic suspensions were given in section 2.3. Among the studied methods, the optimum slips for each material were prepared according to Table 5.1.1. Darvan-C was used as deflocculant in the preparation of alumina suspension. Mostly covered in literature, Dolapix CE–64 was used in the preparation of stable zirconia slurries. However, the interaction of a number of different surfactants (Dolapix G–10, Dolapix SPC–7, Dolaflux SP Neu, Giessfix 162, Dolapix PC 67) with zirconia suspension were investigated by the use of Plackett-Burmann Screening Design and finally Dolapix CE–64 was decided to be used in the preparation of zirconia slurries.

Table 5.1.1. Prepared optimum slip compositions

Type of slip	Alumina slip	Zirconia slip	Alumina-zirconia slip
Solids loading	44.8 vol.%	35.6 vol.%	50 wt.% A + 50 wt.% Z
Type of deflocculant	Darvan-C (Vanderbilt Co. Norwalk, CT, USA)	Dolapix CE-64 (Zschimmer&Schwartz Lahnstein /Germany)	Dolapix CE-64 (Zschimmer&Schwartz Lahnstein /Germany)
Amount of deflocculant	2.6 wt %	1.4 wt %	1.4 wt %

X-ray diffraction analysis of transparent and/or opaque frit is given in Figure 5.1.6. Both frit species displayed amorphous structure as expected. Because frit melts have an easy glass forming composition with a lot of SiO_2 and are quickly cooled during production which further favors glass formation.

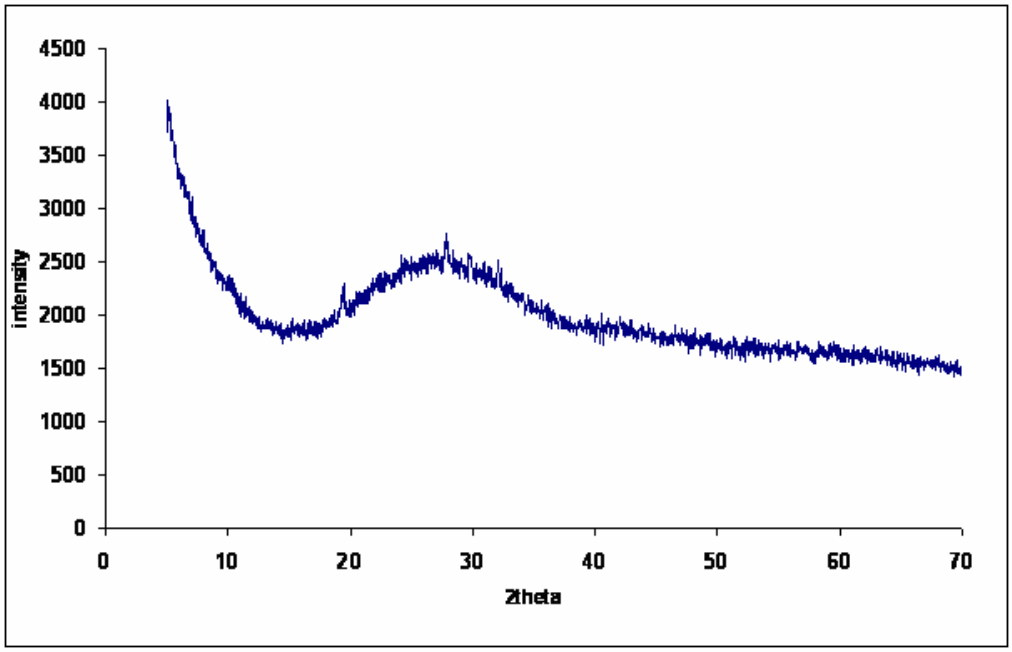

Figure 5.1.6.a XRD pattern of transparent frit

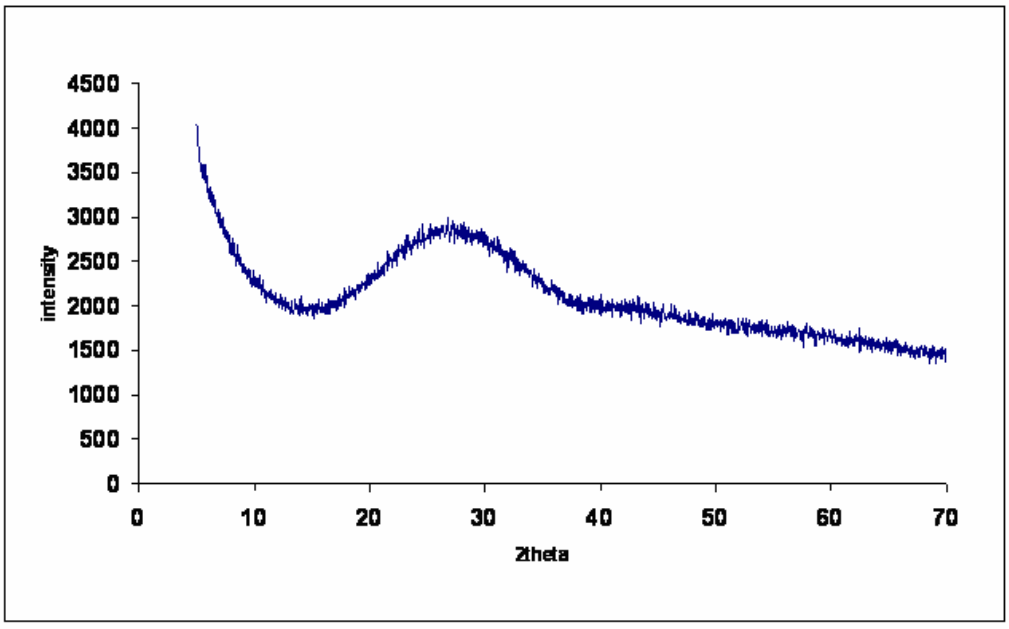

Figure 5.1.6.b XRD pattern of opaque frit

Upon completion of the frit melting experiment, the alumina crucibles and their frit content remained intact with minor cracks in the crucible (Figure 5.1.7.a. and 5.1.7.b.) that probably formed at low temperatures because there was no liquid leaking out through the cracks. Zirconia crucibles, however, were fractured significantly (Figure 5.1.7.c. and 5.1.7.d.) because of thermal expansion mismatch between the frit species (CTE= 4-8 x $10^{-6}/^{0}C$) and ZrO_2 (CTE=9 to $10x10^{-6}/^{0}C$, (Subramanian 1987). However, mixed alumina-zirconia (AZ) crucibles were observed to be resistant to the frit corrosion, due to the continuous nature of the Al_2O_3 phase in the crucible microstructure containing isolated pockets of 2-5 μm ziconia spheres that were probably remnants of starting zirconia granules (Figures 5.1.7.e and 5.1.7.f.).

(a) transparent frit –Al_2O_3 interaction

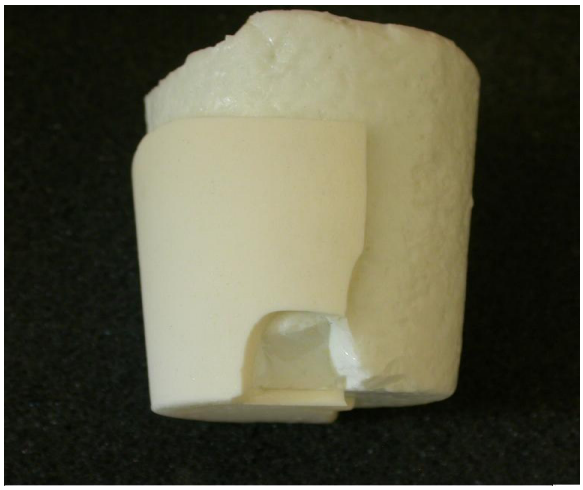

(b) opaque frit –Al_2O_3 interaction

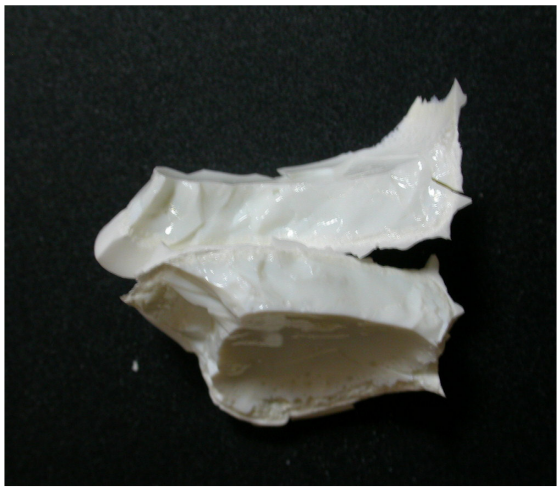

(c)transparent frit- ZrO_2 interaction

(d) opaque frit- ZrO_2 interaction.

(e) transparent frit Al_2O_3-ZrO_2 interaction

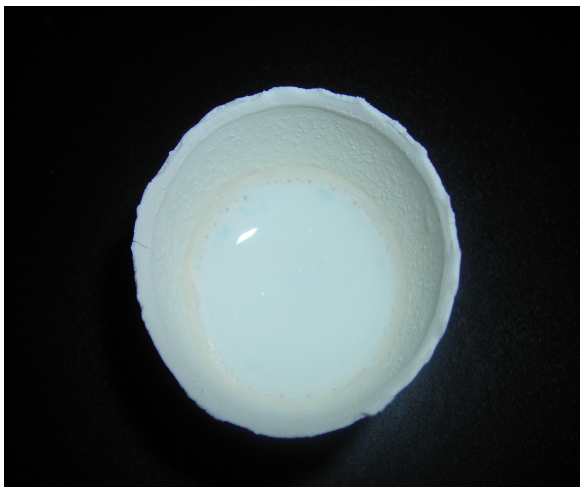

(f) opaque frit Al_2O_3-ZrO_2 interaction

Figure 5.1.7. Digital images representing the frit melt in each tested crucible

5.2. Postmortem Analysis of the Crucible- Frit Interface

Because the crucibles were produced to contain frit melt at high temperature, their behavior in contact with molten frit at high temperature and the interactions along the frit-crucible interface were important. The investigation of the interface formation through Al_2O_3 , ZrO_2 and Al_2O_3-ZrO_2 crucible wall and frit melt was done primarily by optical microscopy, in bright field, cross-polars mode with the DIC, Nomarski filter in, as this filter provides a colored effect to better see the surface relief. The relief effects displayed by the etched surface of the samples are shown in Figure 5.2.1.

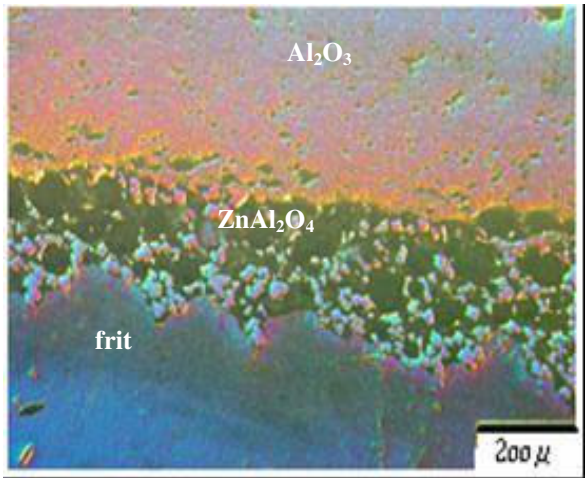

(a) Al_2O_3 crucible wall-transparent frit interface

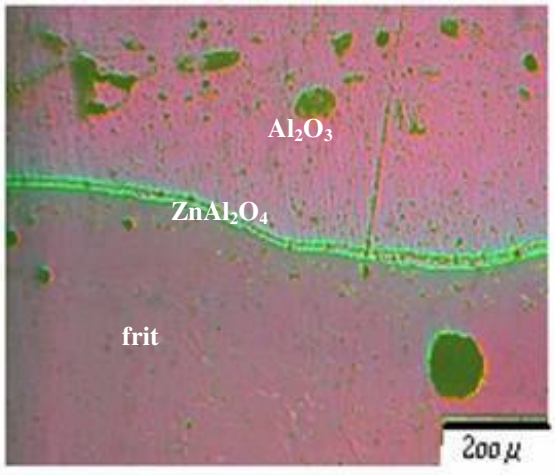

(b) Al_2O_3 crucible wall-opaque frit interface

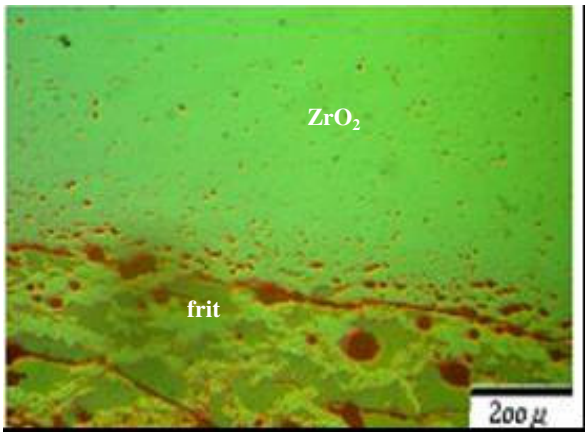

(b) Al_2O_3 crucible wall-opaque frit interface

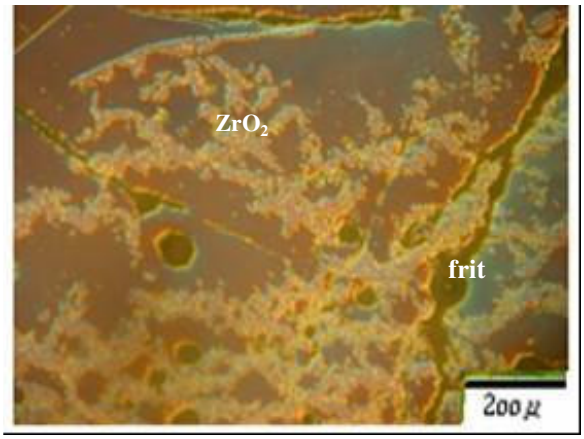

d) ZrO_2 crucible wall-opaque frit interface

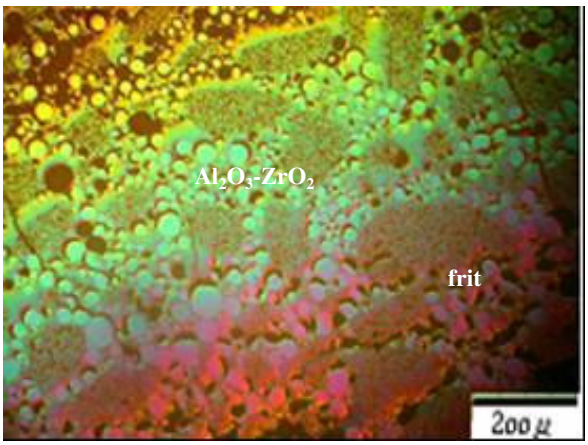

(e)Al_2O_3-ZrO_2 crucible wall-transparent frit interface

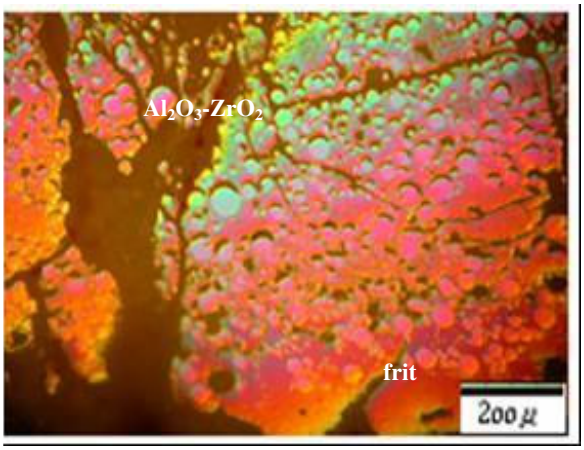

(f) Al_2O_3- ZrO_2 crucible wall-opaque frit interface

Figure 5.2.1. Optical microscopy images of studied refractory – frit interface

Formation of a new phase was only observed in alumina crucible wall – frit interface (Fig 5.2.1.a and b). A continous band of well-crystallized cubic $ZnAl_2O_4$ precipitates was observed along the interface. Alumina from the crucible supplied the aluminum while the frit supplied zinc for the formation of $ZnAl_2O_4$. The presence of this band of $ZnAl_2O_4$ crystals could not be confirmed on Fig 5.2.1.e and f. But SEM analysis indicated that there were widespread precipitations of this new phase along the interface (Fig. 5.2.2. e and f).

In the case of Al_2O_3 crucible use, not much dissolution, a mismatch of thermal expansion coefficients with frit species, 4-8 x 10^{-6} /^oC for frit, and CTE = 8 x 10^{-6}/^oC for alumina "(Subramanian 1987)" respectively and no significant colour change were observed along the crucible wall and frit interface after the runs. However, formation of a new phase along the interface was detected in the SEM study in both transparent and opaque frits (Figures 5.2.2.a and 5.2.2.b). Formed band of new crystals were analyzed by EDX from many sections and the chemical composition of the crystals were identified as $ZnAl_2O_4$ (Figures 5.2.4.a-b). The remaining alumina in this composition was entirely dissolved in the glass phase. As alumina dissolves in the glass, it creates an alumina-saturated glass interface next to the refractory. The band along which $ZnAl_2O_4$ crystals formed was broader in transparent frit (350μm) compared to that in opaque frit (30μm) as the amount of precipitated $ZnAl_2O_4$ depends on the amounts of zinc and aluminium oxides "(Yekta et al. 2007)".

In the case of ZrO_2 crucible use, significant amount of dissolution was observed along the ZrO_2 crucible wall and the frit interface. Frit melts were found to change colour after the runs showing a large amount of ZrO_2 dissolution into frit. Complete wetting of ZrO_2 by frit in Figure 5.2.2.c-d occurred. This material contains zirconia crystals embedded in a glass matrix. Zirconia goes into phase transformation, on cooling ZrO_2 from above 1200 ^oC to room temperature. The tetragonal to monoclinic transformation occurs with a 3 to 5% volume expansion, and develops microcracks around the ZrO_2 particles through which frit penetration becomes easy "(Stevens 1986)". The differences between CTE of transparent frit (4.0 x 10^{-6} /^oC) and zirconia (9-10x 10^{-6} /^oC) led to significant amount of cracks in the lower portion of the crucibles that were in contact with the frit melt on cooling (Figure 5.1.7. c-d).

Figures 5.2.2.e and f show the interface between frit (left) and AZ crucibles (right). The frit consisted of a glassy matrix (gray) in which occasionally ZrO_2 crystal agglomerates were present due to the poor dispersion of ZrO_2 granules in Al_2O_3 during suspension preparation for casting of crucibles. A continous band of $ZnAl_2O_4$ Figures 5.2.2.e and f show the interface between frit (left) and AZ crucibles (right). The frit consisted of a glassy matrix (gray) in which occasionally ZrO_2 crystal agglomerates were present due to the poor dispersion of ZrO_2 granules in Al_2O_3 during suspension preparation for casting of crucibles. A continuous band of $ZnAl_2O_4$ idiomorphic crystals was observed along the interface. Also, EDX analysis confirmed the observed phases throughout the microstructure. The SEM images of the interface that was formed by the melt of frit at temperatures of 1400 and 1450 ^oC within the Al_2O_3 and ZrO_2 crucibles were given in Figure 5.2.3. where the resulting microstructure was not observed to be different from the microstructure developed at 1500 ^oC.

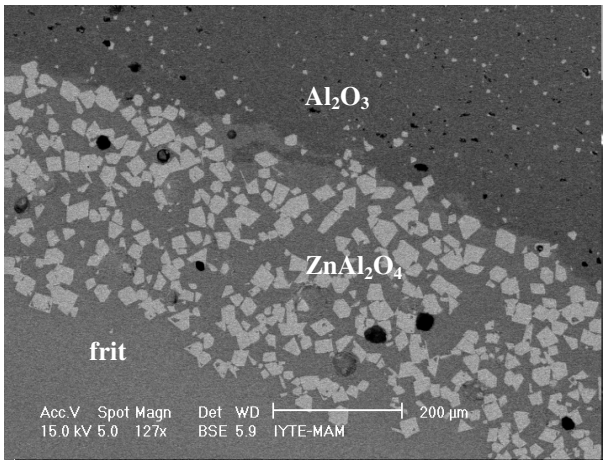

(a) Al_2O_3 crucible wall-transparent frit nterface(1500°C)

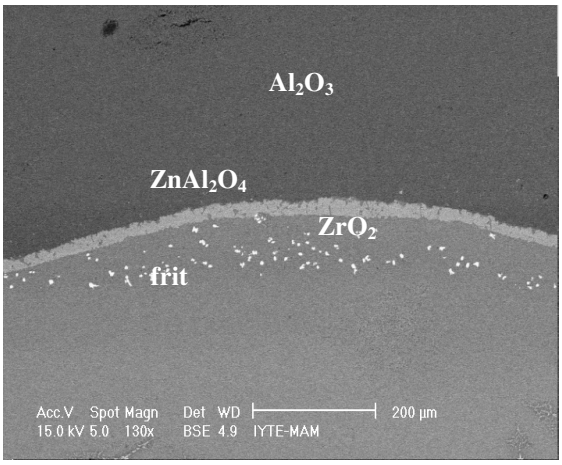

(b) Al_2O_3 crucible wall-opaque frit interface (1500°C)

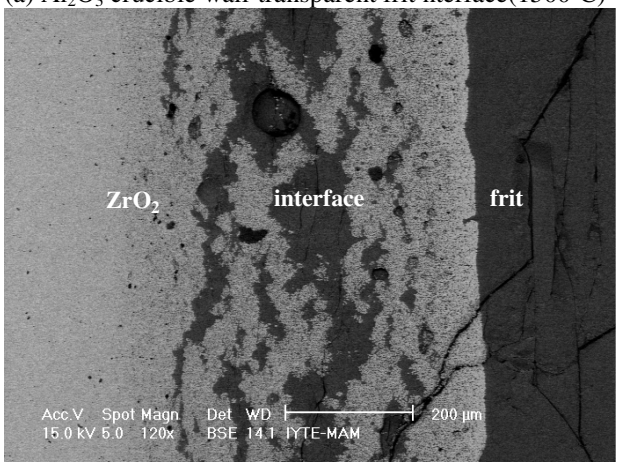

(c) ZrO_2 crucible wall-transparent frit interface(1500°C)

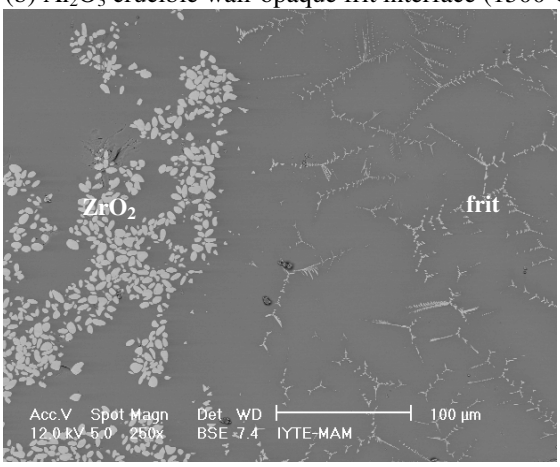

(d) ZrO_2 crucible wall-opaque frit interface(1500°C)

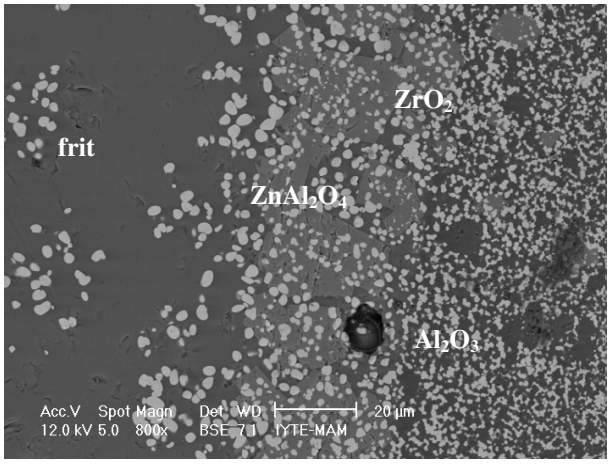

(e) Al_2O_3-ZrO_2 crucible wall-transparent frit interface (1500°C)

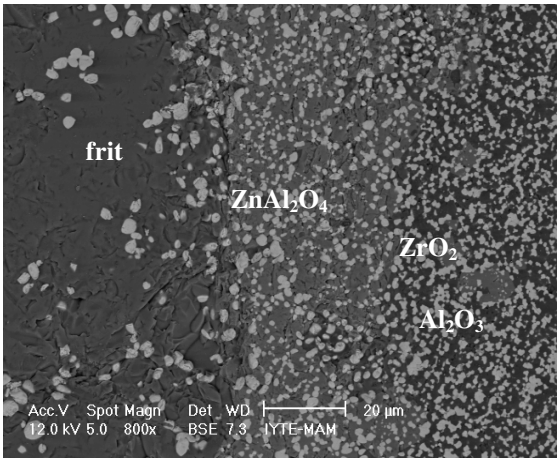

(f) Al_2O_3- ZrO_2 crucible wall-opaque frit interface (1500°C)

Figure 5.2.2. SEM images of studied refractory – frit interface (1500 °C)

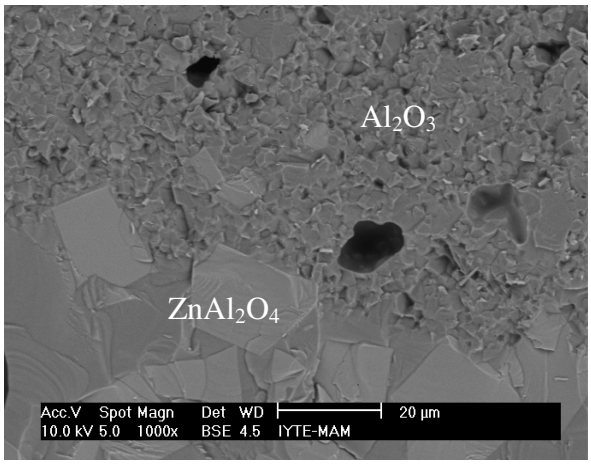

(a) Al_2O_3 crucible wall-transparent frit interface (1450^{o}C)

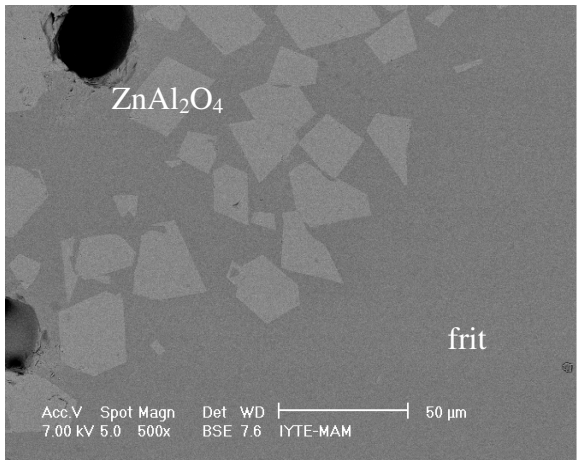

(b) Al_2O_3 crucible wall-opaque frit interface (1450 ^{o}C)

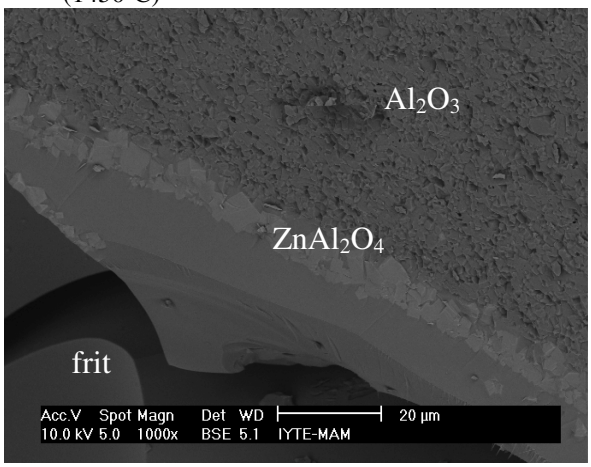

(c) Al_2O_3 crucible wall-transparent frit interface (1400^{o}C)

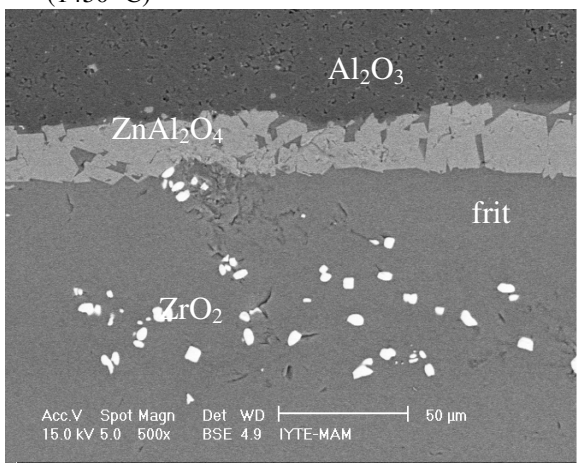

(d) Al_2O_3 crucible wall-opaque frit interface (1400 ^{o}C)

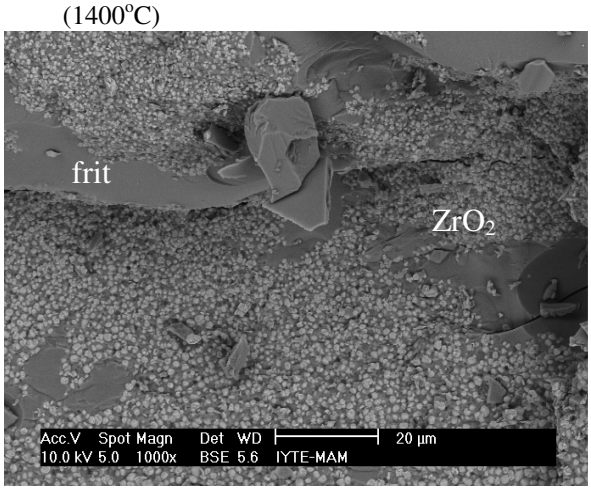

(e) ZrO_2 crucible wall-transparent frit interface (1450^{o}C)

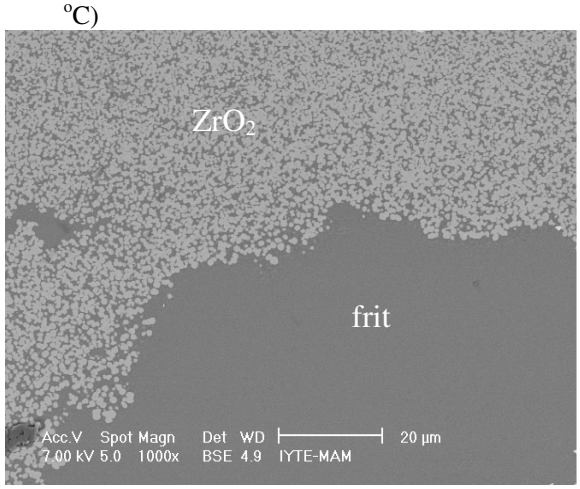

(f) ZrO_2 crucible wall-opaque frit interface(1450^{o}C)

Figure 5.2.3. SEM images of studied refractory – frit interface (1400-1450 ^{o}C)

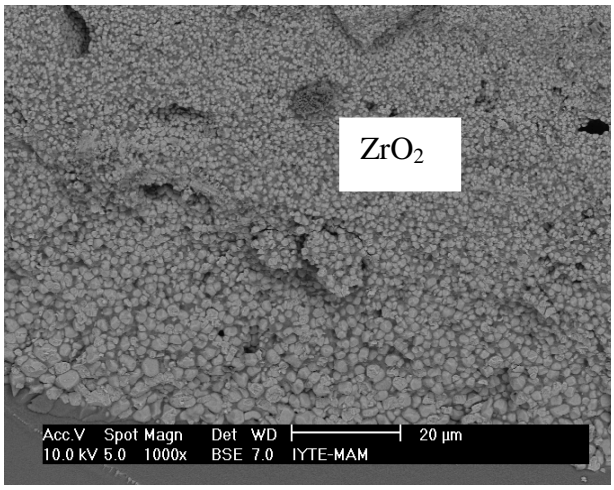

(g) ZrO_2 crucible wall-transparent frit interface (1400°C)

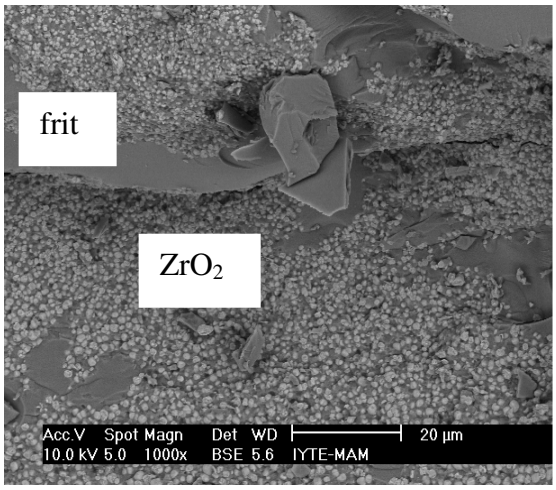

(h) ZrO_2 crucible wall-opaque frit interface(1400°C)

Figure 5.2.3. SEM images of studied refractory – frit interface (1400-1450 °C) **(cont.)**

According to Yekta et al., the precipitation of $ZnAl_2O_4$ (gahnite) in the Li_2O-free glazes can produce an increase in hardness when CaO and MgO are gradually replaced by ZnO "(Yekta et al. 2007)". The below given EDX analysis of the interface formed between the alumina crucible wall-frit confirms that its composition was determined as $ZnAl_2O_4$ (Figures 5.2.4.a–b). Formation of ZrO_2 crystals in opaque frit and incomplete melting of $ZrSiO_4$ away from this interface were also observed (Figures 5.2.4.c–d). When Figures 5.2.4.e-f were investigated, formation of $ZnAl_2O_4$ crystals at the interface of alumina-zirconia crucible wall and frit was obvious. Whereas, large Al_2O_3 crystal formation interjacent to the undispersed ZrO_2 granules and $ZnAl_2O_4$ crystals were clear (Figures 5.2.4.g–h).

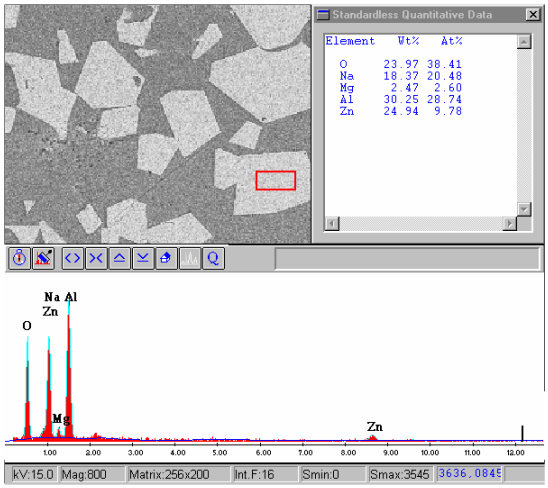

(a) Al_2O_3 crucible wall-transparent frit interface Formation of $ZnAl_2O_4$ crystals

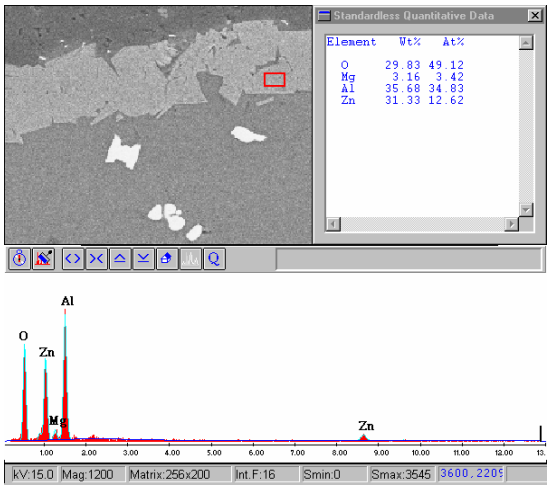

(b) Al_2O_3 crucible wall-opaque frit interface Formation of $ZnAl_2O_4$ crystals

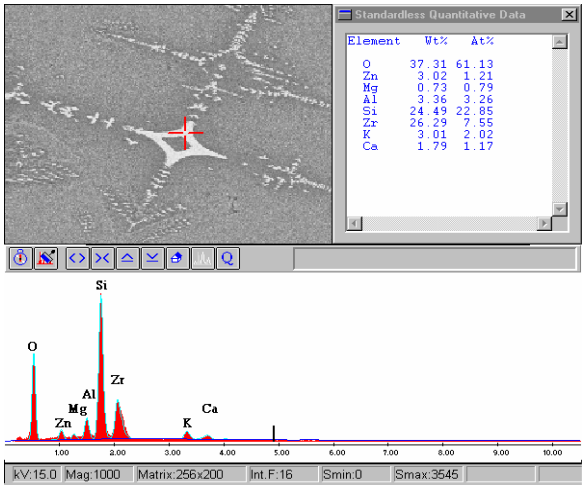

(c) Al_2O_3 crucible wall-opaque frit interface Formation of $ZrSiO_4$ crystals

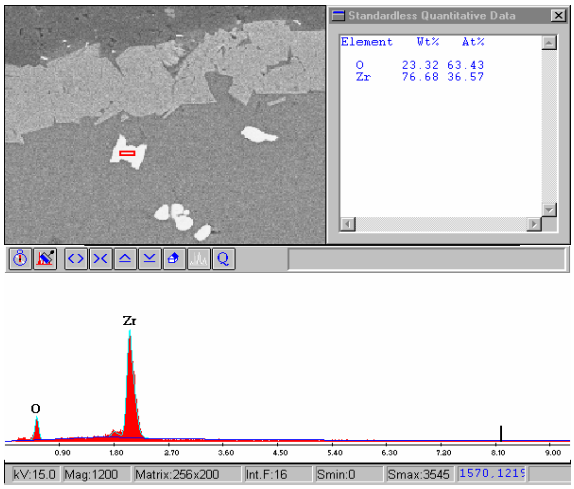

(d) Al_2O_3 crucible wall-opaque frit interface Formation of ZrO_2crystals

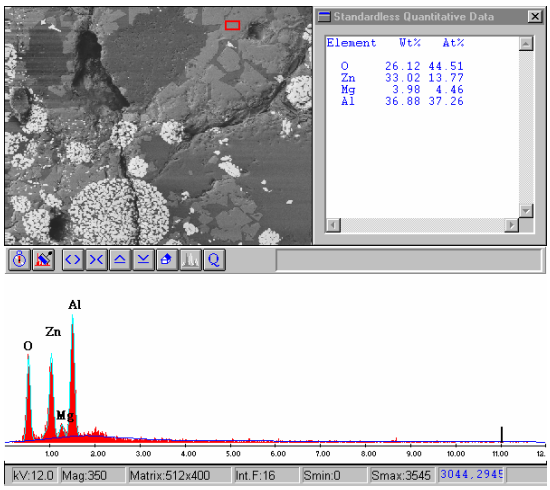

(e) Al_2O_3-ZrO_2 crucible wall-transparent frit interface Formation of $ZnAl_2O_4$ crystals

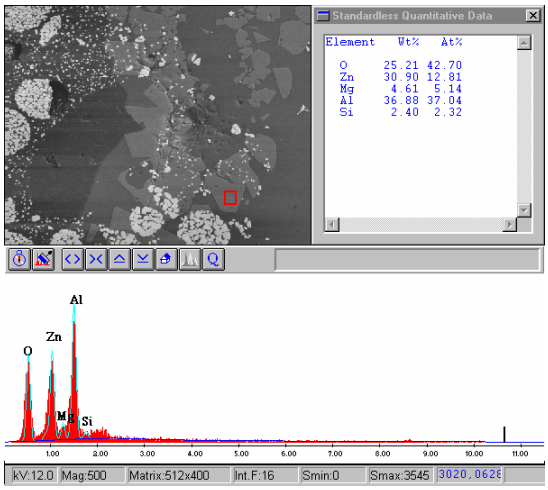

(f) Al_2O_3- ZrO_2 crucible wall-opaque frit interface Formation of $ZnAl_2O_4$ crystals

Figure 5.2.4. EDX analysis of studied refractory – frit interface

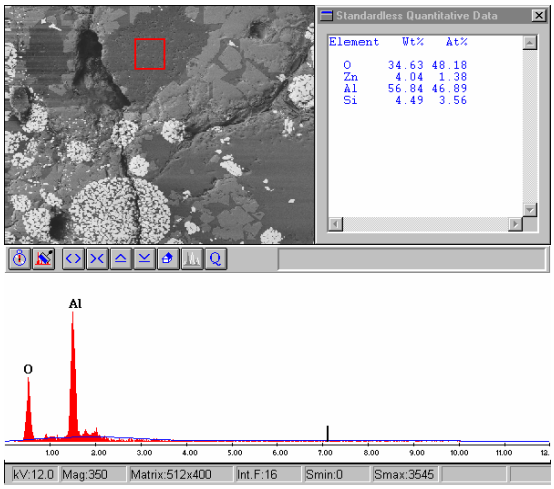

(g) Al_2O_3-ZrO_2cruciblewall-transparent frit interface, Formation of Al_2O_3 crystals

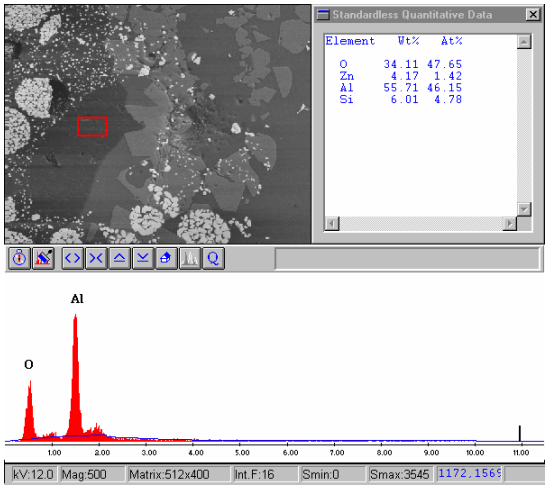

(h) Al_2O_3- ZrO_2 crucible wall-opaque frit interface Formation of Al_2O_3 crystals

Figure 5.2.4. EDX analysis of studied refractory – frit interface **(cont.)**

The proportions of the elements displayed by EDX results helped confirm the identity of the newly formed phases at the interface and throughout the frit matrix.

Alumina and zirconia were tested as potential materials for making crucibles to be used for containing transparent and/or opaque frit. Test results indicated that alumina could satisfactorily perform well in corrosion tests. Therefore, further tests were performed for alumina crucible in order to investigate the nature of the congruity with the frit species.

X-ray diffraction (Phillips X'Pert Pro) was used to determine the crystalline phases formed at the interface and to comprehend the mechanisms of dissolution between the species. A tested crucible specimen containing a solidified frit melt was sectioned and carefully ground to remove frit from the specimen surface in order to eliminate the frit part and just leave the interface for analysis of the $ZnAl_2O_4$ formation by XRD (Figure 5.2.5.). This was done to confirm the initial finding in EDX analysis that offered the presence of $ZnAl_2O_4$.

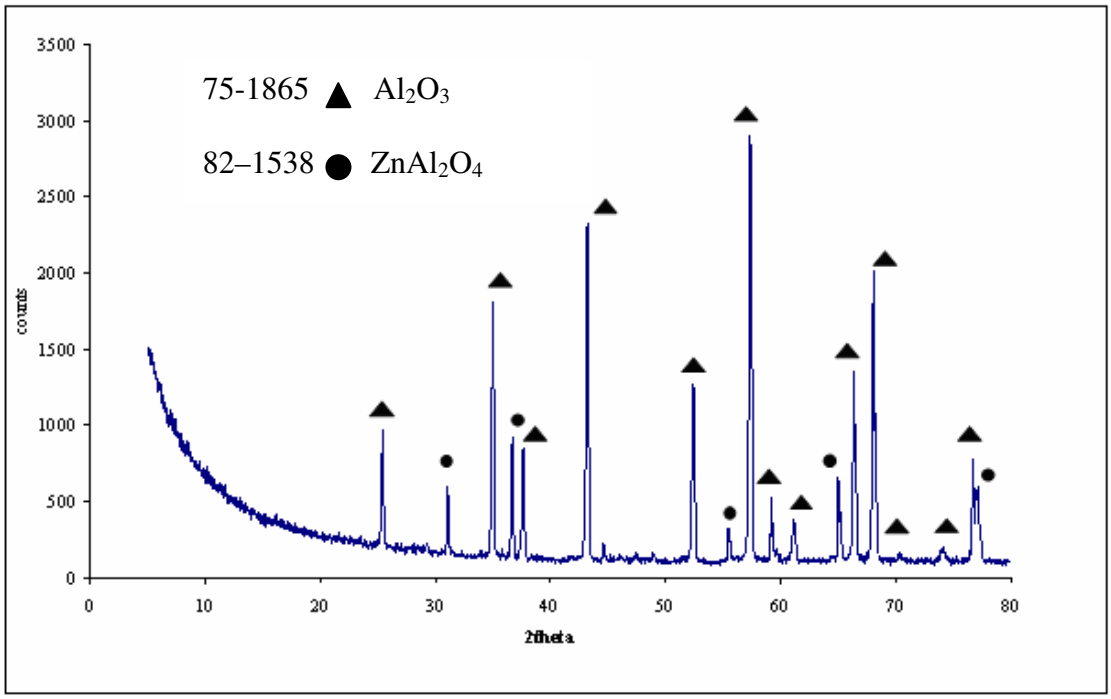

Figure 5.2.5. XRD pattern of Al_2O_3-frit interface after removal of excess frit from the surface of the crucible by grinding.

When designing crucibles for use at elevated temperatures it is important that the crucible does not dissolve into the melt to a large extent which might jeapordize the quality of the corrosion test. The concentration gradient between the refractory test specimen and the frit melt might change during the test. EDX analysis give northworthy data about the dissolution and loss of the constituents present in the frit in relation to the original frit before testing. Not much change was observed in the composition of the frit melted in alumina crucible compared to the original one (Table 5.2.1). The new frit composition was not enriched by Al element in huge amounts and this shows that not much Al dissolution from Al_2O_3 crucible in contact with the glass occured. (Figure 5.2.6.a-d.).

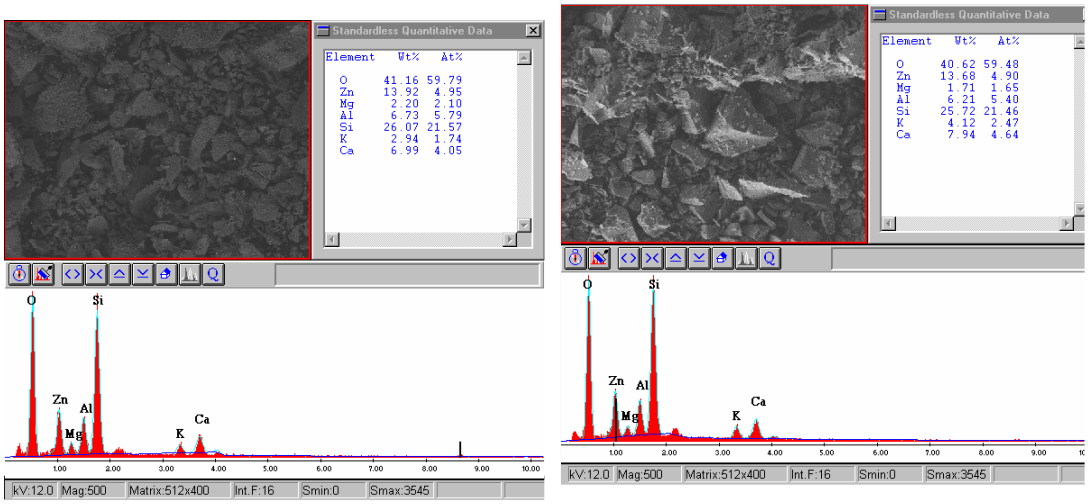

(a) original transparent frit (b) molten transparent frit (1500 °C)

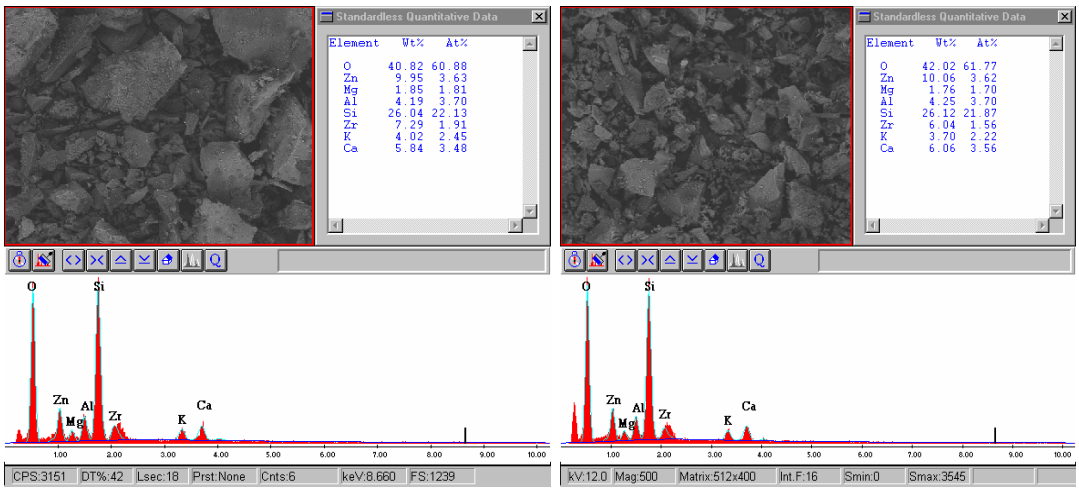

(c) original opaque frit (d) molten opaque composition (1500 °C)

Figure 5.2.6. EDX analysis of original and molten transparent and/or opaque frit species

Table 5.2.1. EDX analysis of original and melted transparent and/or opaque frit

Element	**Original transparent frit**		**Melted transparent frit**		**Original opaque frit**		**Melted opaque frit**	
	wt%	at%	wt%	at%	wt%	at%	wt%	at%
O	41.2	59.8	40.7	59.5	40.8	60.9	42.0	61.8
Zn	14.0	5.0	13.7	5.0	10.0	3.6	10.1	3.6
Mg	2.2	2.1	1.7	1.7	1.8	1.8	1.8	1.7
Al	6.7	5.8	6.2	5.47	4.2	3.7	4.3	3.7
Si	26.1	21.6	25.7	21.5	26.0	22.1	26.1	22.0
K	3.0	1.7	4.1	2.5	4.0	2.5	3.7	2.2
Ca	7.0	4.0	8.0	4.6	5.8	3.5	6.1	3.6
Zr	0.0	0.0	0.0	0.0	7.3	1.9	6.0	1.6

CHAPTER 6

CONCLUSIONS AND RECOMMENDATIONS

Al_2O_3 and ZrO_2 crucibles were successfully produced. They were chemically homogeneous, mechanically sound and free from pores. When in contact with a commercial frit melt at high temperature (1400-1500^oC) their chemical interaction with the frit melt yielded the following findings:

- Zirconia crucibles were not chemically resistant to frit melts contrary to expected predictions from phase diagram studies. This was probably due to wetting effects that led to complete penetration and ingress of frit into the zirconia crucible wall.
- Zirconia crucibles were found to fracture upon cooling due to thermal expansion mismatch between zirconia (9-10x10^{-6} /^oC) and frit (4-8x10^{-6} /^oC).
- Zirconia powder of average particle size of 0.5 μm was used in granular form and the SEM images pointed out that these granules could not be perfectly dispersed. This may perhaps lead to incomplete mixing of the slip.
- Alumina crucibles were chemically resistant to frit attack and little dissolution of alumina was observed into the frit. This small amount of dissolution (<3%) was satisfactory as far as the validity of the corrosion test was concerned.
- Al_2O_3 - ZrO_2 (AZ) crucibles performed successfully, behaving more like the alumina crucibles.
- In the case of Al_2O_3 crucible use, with both frit species, $ZnAl_2O_4$ formation was observed at the interface where the width of the band of $ZnAl_2O_4$ differed significantly mostly dependent on the amount of the two major oxides (ZnO and Al_2O_3) in each frit composition. Also, presence of ZrO_2 in opaque frit was observed adjacent to the $ZnAl_2O_4$ band.
- Crystallization of $ZrSiO_4$ was another finding in the opaque frit region with respect to the natural opaque frit composition. On the other hand, in Al_2O_3-ZrO_2 crucible wall-frit interface, beside the presence of $ZnAl_2O_4$ crystals, large Al_2O_3 crystals were apparent. Upon incomplete dispersion of ZrO_2 in prepared Al_2O_3-ZrO_2 suspension, huge granule shaped zirconia crystals were evident.

The use of modified frit compositions in melting processes, utilization of different types of powder forms of Al_2O_3 and ZrO_2 materials in the production of crucibles, experimentation of melting behaviours of other process liquids in the same type of ceramic crucibles for evaluating their corrosion resistance can be studied as the future work. Also additional experimental study on the preparation of stable Al_2O_3-ZrO_2 suspensions for producing AZ crucibles should be conducted.

REFERENCES

Akamatsu Takeshi, 1983. "Continuous Fabrication of a Phosphate Glass Fiber", *Journal of Lightwave Technology*, Vol.1, No: 4, pp: 48-52.

Aksel Cemail, 2003. "The Microstructural Features of an Alumina-Mullite-Zirconia Refractory Material Corroded by Molten Glass", *Ceramics International*, Vol: 29, pp.305-309.

Alcoa Industrial Chemicals, 2007. Product Data, Calcined and Reactive Aluminas for the Ceramic Industry, Frankfurt.

Asokan T., 1994. "Microstructural Features of Fusion Cast Al_2O_3-ZrO_2-SiO_2 Refractories", *Journal of Materials Science Letters*, Vol: 13, pp.343-345.

Barbieri L., Corrodi A., Lancelotti I., Leonelli C., Siligardi C., 2002. "Glass Formation and Devitrication in the K_2O-ZrO_2-SiO_2 System", *Physics and Chemistry of Glasses*, 43C.

Briscoe J. Brian, Khan U.Asad and Luckham F. Paul, 1998. "Optimising the Dispersion on an Alumina Suspension Using Commercial Polyvalent Electrolyte Dispersants", *Journal of the European Ceramic Society*, Vol: 18, pp. 2141-2147.

Bunshah R.F., 1968. "*Technique of Materials Preparation and Handling, Part I*", Interscience, New York.

Bunting E.N., 1956. "*J.Research Natl.Bur.Standard"*, Vol. 2 in Phase Diagrams for Ceramists, Ed. Margie K. Reser, pp. 151, OH.

Chen Ming, Hallstedt Bengt, Gauckler Ludwig J., 2004. "Thermodynamic modeling of the ZrO_2–$YO_{1.5}$ system", *Solid State Ionics*, pp. 255–274.

Dos Santos Ieda Maria Garcia, Martins Moreira Rafael Carlos, 2003. "Ceramic Crucibles: a new alternative for melting of PbO-BiO1.5-GaO1.5", *Journal of Non-Crystalline Solids*, Vol. 319, pp.304-310.

Dunkl Michael, Gupta Amil and Mackintosh Joe, 2003. "Considerations of the Corrosion of Refractories by Glass", *Glass*, August issue.

Eppler Richard A. and Eppler Douglas R., 2000. *"Chapter 3: Formulation of Glazes",* in Glazes and Glass Coatings, published by the American Ceramic Society, pp. 29-71 and pp. 104-252, Westerville, Ohio.

Fengqiu Tang, Xiaoxian Huang, Yufeng Zhang and Jingkun Guo, 1998. "Effect of Dispersants on Surface Chemical Properties of Nano-Zirconia Suspensions", *Ceramics International*, Vol: 26, pp.93-97.

Fontana Mars G., 1986. *"Corrosion Engineering"*, Ed. McGraw-Hill International Editions, pp. 57, Materials Science and Engineering Series, New York.

Fredericci C., Zanotto E.D., Ziemath E.C., 2000. *Journal of Non-crystalline Solids*, Vol. 273, pp. 64.

Funk James E. and Dinger Dennis R., 1993. "*Chemical Additives for Forming Processes*" in Predictive Process Control of Crowded Suspensions Applied to Chemical Manufacture, Vol: 1, Ed. JEFCO Ceramic Consultants, pp.229-230, Seneca.

Garrido L.B., Aglietti E.F., 2001. "Pressure Filtration and Slip Casting of Mixed Alumina-Zircon Suspensions", *Journal of the European Ceramic Society*, Vol: 21, pp.2259-2266.

J.T. Jones and M.F. Berard, 1993. *"Ceramics Industrial Processing and Testing"*, II. Edition, Iowa State University Press, AMES, Iowa, pp.6-23, pp.70-105.

K. Subramanian and S. Ramanath, 1987. "*Principles of Abrasive Machining*", in Engineered Materials Handbook, Vol:4 Ceramics and Glasses, Ed. S.J. Schneider, pp. 316, ASM International, Materials Park, OH.

K.A. Maskall and D.White, 1986. "*Vitreous Enamelling*", by Oxford Pergamon Press.

Kingery W.D., 1960. "*Ceramic Processes and Products*", in Introduction to Ceramics II. Edition, Ed. John Wiley & Sons, pp. 10-14, New York.

Kunes Karel, Havrda Jiri, Hronikova Katerina, Gregorova Eva and Pabst Willi, 1999. " Stabilization of Bioceramic Suspensions Prepared From Alumina-Containing Zirconia Powders", 2000, *Ceramics-Silikaty* Vol: 44, pp.1-8.

Lecomtea G., Pateyronb B., Blancharta P., 2004. "Experimental study and simulation of a vertical section mullite-ternary eutectic (985 ^{o}C) in the SiO_2–Al_2O_3–K_2O system", *Materials Research Bulletin,* Vol: 39, pp.1469–1478.

Lee W.E. and Hawksworth A., 1996. "Microstructural Observation of Bottom-drilling Corrosion in Electrocast Al_2O_3-ZrO_2-SiO_2 Refractories", *Journal of Materials Science Letters*,Vol: 15, pp.1702-1704.

Lee William E. Phil D. and Rainforth W. Mark, 1994. "*Ceramic Microstructures, Property Control by Processing*", published by Chapman & Hall, (London, UK), pp. 28-29.

Leigh David H., Towe Carey A., 1987. "Use of a Screening Experimental Design to Develop a High Al_2O_3 Casting Slip", *Ceramic Bulletin*, Vol.66, pp. 786-789.

Leong Yee-Kwong and Boger David V., 1990. "Surface Chemistry and Rheological Properties of Zirconia Suspensions", 1991, *The Society of Rheology*, Inc., Vol: 35 (1).

Manfredo L.J. and McNally R.N., 1984. "The Corrosion Resistance of High ZrO_2 Fusion-cast Al_2O_3-ZrO_2-SiO_2 Glass Refractories in Soda Lime Glass", *Journal of Materials Science*, Vol: 19, pp.1272-1276.

Mattson Einar, 1989. "*Basic Corrosion Concepts*" in Basic Corrosion Technology for Scientists and Engineers, Ellis Harwood Series in Corrosion and Its Preventation Ed. A. D. Mercer, pp. 29-47, Chichester.

Mazer James J., Bates John K., Biwer Bruce M., and Bradley Charles R., 1991. "AEM Analyses of SRL 131 Glass Altered as a Function of SA/V", *Materials Research Society Meeting Scientific Basis for Nuclear Waste Management XV,* Strasbourg, France.

McCauley Ronald A. 1995. "*Corrosion, a Rewiev of Some Fundamentals*", Corrosion of Materials by Molten Glass, Ceramic Transactions, Vol. 78, edited by George A. Pecoraro, James C. Marra, John T. Wenzel, pp.81-89, OH.

Morelli M.R. and Fredericci C., 2000. "Corrosion of AZS and AZ Crucibles in Contact With a Blast- Furnace Slag-Based Glass", *Materials Research Bulletin*, Vol. 35, pp. 2503-2514.

Mutsuddy Beebhas C., 1987. "*Engineering Properties of Zirconia*", in Engineered Materials Handbook, Vol:4 Ceramics and Glasses, Ed. S.J. Schneider, pp. 173-180, ASM International, Materials Park, OH.

Nishikawa Akira, 1984, "Section: 3 Corrosion" in *Technology of Monolithic Refractories*, Vol. 1, edited by Plibrico Japan Company Limited, pp. 212-224, Minato-ku, Tokyo.

Omatete O.O. and Janney,M.A., 1992. "Method for Molding Ceramic Powders Using A Water-Based Gel Casting", U.S. Pat. No. 5 028 362, 1991, and U.S. Pat. No. 5 145 908.

Osborn E.F., Muan A., 1960. "Phase Equilibrium Diagrams of Oxide Systems", The American Ceramic Society and The Edouard Orton Jr. Ceramic Foundation, Columbus, OH.

Poirier J., Qafssaoui F., Ildefonse J. P. and Hubert P., 2004. "Influence of the Liquid Phase on the Slag Corrosion of Andalusite Based Refractories", *Refractories Applications Transactions*, Vol.1, No.1.

Popa A.M., Vleugels J., Vermant J., Van der Biest O., 2006. "Influence of Surfactant Addition Sequence on the Suspension Properties and Electrophoretic Deposition Behaviour of Alumina and Zirconia", *Journal of the European Ceramic Society*, Vol.26, pp. 933-939.

Pradhan Mamata and Bhargava Parag, 2005. "Influence of Sucrose Addition on Rheology of Alumina Slurries Dispersed with a Polyacrylate Dispersant", *Journal of American Ceramic Society*, Vol: 88, pp.833-838.

Pretorius G., 1995. "Applied Solid state Chemistry of Zircon and Zirconia, PhD Thesis", Institute for Applied Materials, University of Pretoria, pp. 9-14.

R. Stevens, 1987. "*Engineering Properties of Zirconia",* in Engineered Materials Handbook, Vol:4 Ceramics and Glasses, Ed. S.J. Schneider, pp. 775-786, ASM International, Materials Park, OH.

Reed J.S., 1995. *"Rheology of Saturated Systems (Slurries and Pastes)",* in Principles of Ceramic Processing II. Edition, Ed. John Wiley & Sons, pp. 277, New York.

Richerson W. David, Ceramatec Inc. Forming and Predensification, *Ceramics and Glasses, Engineered Materials Handbook*, 2000. Vol.4, pp: 123-129.

Ruh R. and Rockett,T.J. 1970. " *The One –Component System*" in Introduction to Phase equilibria in Ceramics, Ed. *The American Ceramic Society*, pp. 17, Westerville, OH.

Sarraf Hamid, 2003. "Comparison of the Rheological Properties of Zirconia Slurries Applied for Slip-cast Ceramics", Institute of Chemical Technology of Prague.

Sarraf H. and Havrda J., 2004. "A Novel Prediction Method for Preparation and Microstructure Developing of Zirconia Ceramics by Colloidal Processing", *Annual Transactions of the Nordic Rheology Society*, Vol. 12.

Schairer J. F. and Bowen N.L., 1956. "*American. Journal of Science*", Vol. 245, in Phase Diagrams for Ceramists, Ed. Margie K. Reser, pp.199- 201, OH.

Singh P. Bimal, Bhattacharjee Sarama, Besra Laxmidhar, Sengupta K. Dilip, "Evaluation of Dispersability of aqueous Alumina suspension in Presence of Darvan C", 2004. *Ceramics International*, 30, pp. 939-946 *Society*, Vol: 27, pp. 2311-2315.

Taylor J. R. and Bull A.C., 1986. *"Ceramics Glaze Technology"*, (Oxford Pergamon Press).

Tsetsekou, Agrafiotis A., Leon C., I. and Milias A., 2001. "Optimisation of the Rheological Properties of Alumina Slurries for Ceramic Processing Applications, Part II: Spray-Drying", *Journal of European Ceramic Society*, Vol. 21, pp.493-506.

WEB_1, 1997 http://www.keram.se/eng/pdf/slip_casting.pdf, 12.08. 06.

WEB_10,2007. http://www.corrosion.ksc.nasa.gov/, 24.06.07.

WEB_2, 2007. http://www.octane.nmt.edu/waterquality/corrosion , 23.06.0.

WEB_3, 2007. http://www.maverickinspection.com, 23.06.07.

WEB_4, 2007. http://www.ksc.nasa.gov/crevcor.htm, 24.06.07.

WEB_5, 2007. http://www.copper.org, 24.06.07.

WEB_6, 2007. http://www.gug.selective.dk/tutorials/rong1/, 24.06.07.

WEB_7, 2007. http://www.chemistryexplained.com/images/chfa, 24.06.07.

WEB_8, 2007. http://www.corrosion.lab.com, 24.06.07.

WEB_9, 2007. http://www. corrosion-doctors.org, 24.06.07.

WEB_11, 2007. http://www. ttiev.com/images/corrosion, 25.06.07.

WEB_12, 2007. http://www.refractoriesinstitute.org/aboutrefractories.htm, 22.03.06.

Yekta Eftekhari B., Alizadeh P., Rezazadeh L., 2007. "Synthesis of Glass-ceramic Glazes in the ZnO-Al_2O_3-SiO_2-ZrO_2 System", *Journal of the European Ceramic Society*, Vol: 27, pp. 2311-2315.

Zhang Jingxian, Xu Qiang, Tanaka Hideaki and Iwasa Mikio, 2006. "Improvement of the Dispersion of Al_2O_3 Slurries Using EDTA-4Na", *Journal of American Ceramic Society*, Vol: 89, [4], pp. 1440-1442.